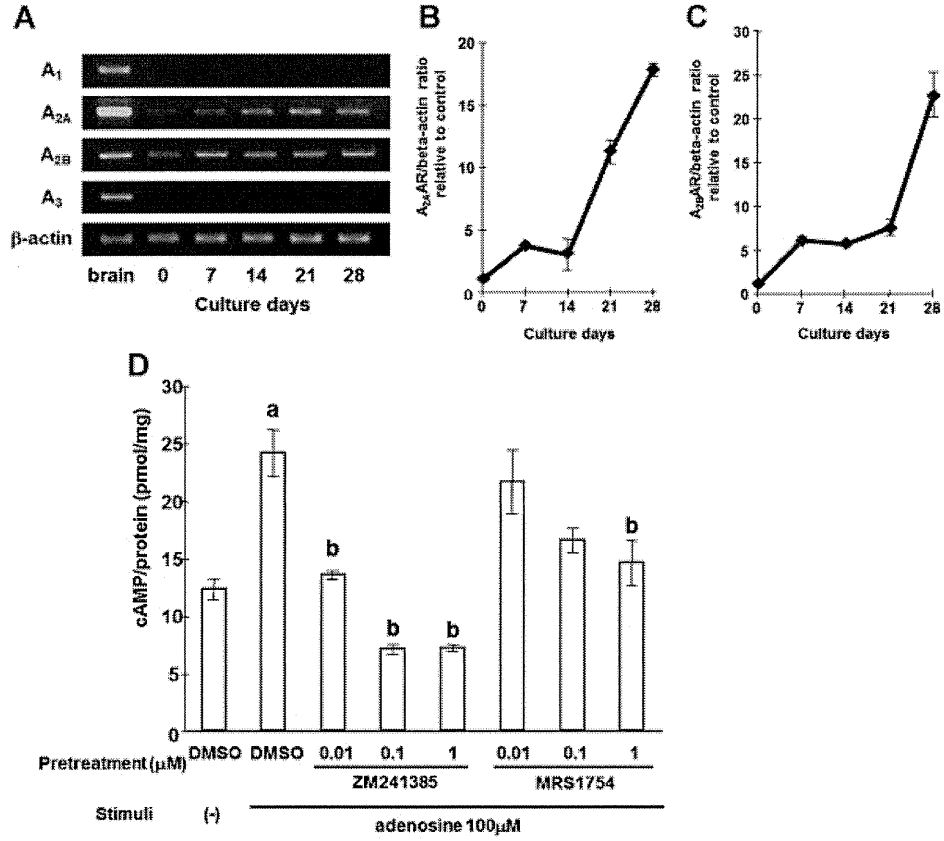

Fig. 5. Expression and function of A_{2A}AR and A_{2B}AR on MC3T3-E1 cells. A: AR mRNA expression during differentiation. MC3T3-E1 cells were cultured in mineralization medium and total RNA was extracted on the indicated days. Expression of AR mRNA was detected by RT-PCR. Mouse brain was used as a positive control for all AR subtypes. B,C: Quantification of A_{2A}AR and A_{2B}AR mRNA expression during osteoblast differentiation by real-time RT-PCR. D: Functional expression of A_{2A}AR and A_{2B}AR. MC3T3-E1 cells were cultured with mineralization medium for 14 days. Cells were then stimulated with exogenous adenosine (100 μM) with or without 5 min pretreatment with the indicated concentrations of ZM241385 (A_{2A}AR antagonist) or MRS1754 (A_{2B}AR antagonist) or DMSO. The DMSO concentration in each well was 0.1%. After 5 min incubation, cells were homogenized and cAMP was measured. $^{a}P < 0.05$ compared with DMSO only. $^{b}P < 0.05$ compared with DMSO and adenosine. Representative results from more than three experiments are shown.

CD73-induced alterations in osteoblast differentiation. As shown in Figure 6A,B, enhanced gene expression of BSP and OC in MC/CD73 was significantly suppressed by treatment with an A_{2B}AR antagonist. Surprisingly, an A_{2A}AR antagonist had no effects on the BSP and OC gene expression of MC/CD73. It is important to note that A_{2A}AR and A_{2B}AR mRNA expression on MC3T3-E1 was not changed by over expression of CD73 (data not shown). These data suggest that CD73-generated adenosine modulates osteoblast differentiation and function via activation of A_{2B}AR.

Discussion

Adenosine has a plethora of biological actions on a large variety of cells and modulates their function. Cells responsible for bone remodeling are no exception. In vitro and in vivo studies demonstrated that formation and function of osteoclasts responsible for bone resorption require A_1AR signaling (Kara et al., 2010a,b). In vitro studies showed proliferation and differentiation of osteoblasts responsible for bone formation could be modulated by AR signaling (Shimegi, 1998; Fatokun et al., 2006; Costa et al., 2010, 2011). Extracellular adenosine which activates AR is generated, at least in part, by ecto-5′-nucleotidse: CD73. The expression of this molecule is regulated by the canonical Wnt and HIF-1α pathways, crucial signaling cascades in bone forming cells (Synnestvedt et al., 2002; Spychala and Kitajewski, 2004). Thus, the possibility that CD73 could impact osteoblast function by modulating nucleotide metabolism and adenosine concentrations prompted us to examine the role of this molecule in bone metabolism.

Significantly decreased serum OC and suppressed osteoblastic gene expression in bone of male *cd73*$^{-/-}$ mice suggest that their reduced bone volume is due to, at least in part, to a defect of osteoblast function (Fig. 2). As CD73 plays a major role in extracellular adenosine generation, this is the first report indicating the involvement of endogenous adenosine in osteoblast function in vivo. A better understanding of the specific role of adenosine can be gained by a detailed analysis of the phenotype observed in *cd73*$^{-/-}$ mice. Unlike cortical bone, trabecular bone volume, and trabecular thickness were significantly reduced (29.5% and 17.9% reduction, respectively), in *cd73*$^{-/-}$ mice as compared to wild-type mice. Likewise, bone mineral density was significantly reduced in the trabecular rich metaphysis but was not statistically reduced in cortical bone. These findings suggest bone microenvironmental-specific

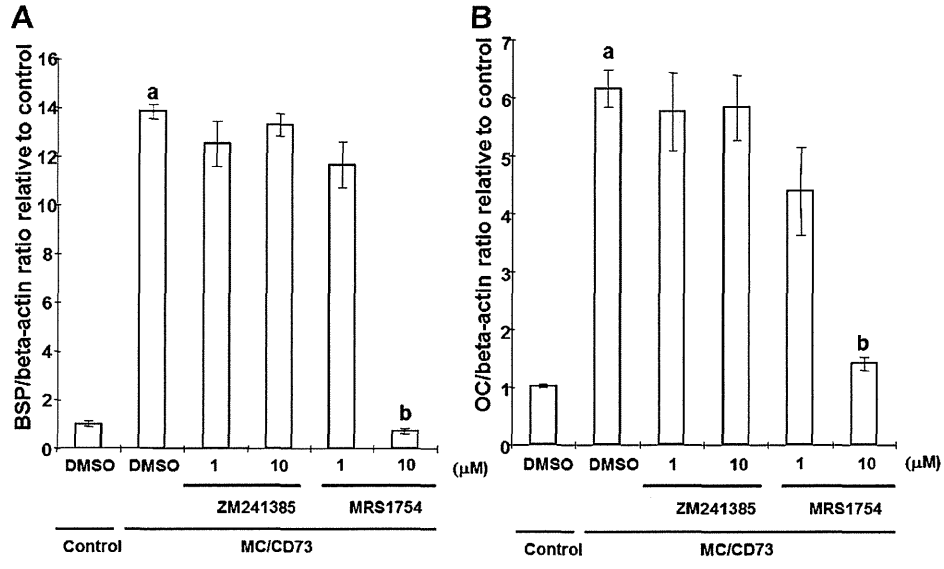

Fig. 6. Involvement of A2BAR signaling in osteoblast differentiation. Suppressive effect of an A_{2B}AR antagonist on (A) BSP and (B) OC mRNA expression in MC/CD73 cells. MC/CD73 cells were cultured for 3 days in α-MEM supplemented with 10% FBS in the presence of the indicated concentration of ZM241385 (A_{2A}AR antagonist) or MRS1754 (A_{2B}AR antagonist) or DMSO only. The DMSO concentration in each well was 0.1%. The expression of BSP and OC were determined by real-time RT-PCR. $^{a}P < 0.05$ compared with DMSO-treated control transfectants. $^{b}P < 0.05$ compared with DMSO-treated MC/CD73 cells. Representative results from more than three experiments are shown.

(trabecular vs. cortical regions) requirements for CD73. Additionally, whole mount staining with alcian blue and alizarin red of E18.5 fetal skeletions, revealed no significant abnormalities between *cd73*$^{-/-}$ and wild-type embryos (data not shown). These data reveal that CD73 is not required for embryonic bone patterning or initial bone formation but is most likely required for bone remodeling that occurs with age. In this study, we showed that CD73 deficiency resulted in osteopenia in male mice but not in female mice at 13 weeks of age. Mature male and female mice are known to show different bone status and remodeling rates. Thus, there may be an interaction between CD73-generated adenosine and one or more age-dependent factors such as sex hormones. Exploring this interaction will be a topic of future work.

In this study, a series of in vitro studies revealed that CD73 promoted osteoblast differentiation, consistent with earlier reports indicating that AR activation regulated proliferation and differentiation of osteoblasts in vitro (Shimegi, 1998; Costa et al., 2011). The relatively modest bone phenotype of *cd73*$^{-/-}$ mice may be due to redundant pathways of adenosine production such as via cytoplasmic nucleotidases or S-adenosyl homocysteine hydrolase. As it is possible that some of these pathways could be up regulated as a consequence of life-long CD73 deficiency, it would be interest to compare the bone phenotype in mice with conditional CD73 deficiency when they become available.

Unlike previous reports suggesting that adenosine supports osteoclast formation and bone resorption (Evans et al., 2006; Kara et al., 2010a,b), we found osteoclast markers were normal in *cd73*$^{-/-}$ mice in the steady state (Fig. 2A) and TRAP staining of tibia showed comparable osteoclast numbers in wild-type and *cd73*$^{-/-}$ mice (data not shown). However, CD73-generated adenosine may modulate osteoclast formation and function during inflammatory bone diseases such as rheumatoid arthritis and periodontitis, because inflammatory cytokines are capable of inducing CD73 expression (Kalsi et al., 2002; Niemelä et al., 2004) and adenosine is a well-known anti-inflammatory mediator (Haskó et al., 2008; Blackburn et al., 2009). Future studies utilizing *cd73*$^{-/-}$ mice in experimental bone disease models will give us more insight into the role of CD73 and endogenous adenosine in the pathogenesis of these diseases.

Elevation of A_{2A}AR and A_{2B}AR expression was observed during osteogenic differentiation (Fig. 5). These subtypes of AR are coupled with Gs proteins that can initiate signaling to stimulate bone formation (Sakamoto et al., 2005; Hsiao et al., 2008). Interestingly the positive role of CD73 on osteoblast differentiation in vitro was mediated by the A_{2B}AR but not the A_{2A}AR (Fig. 6A,B). Our experiments do not rule out the possibility that the A_{2A}AR functions in osteoblast differentiation in vivo independently of CD73; additional experiments with gene-targeted mice will be necessary to address this issue. Based on our data, we hypothesize that CD73-generated adenosine stimulates the A_{2B}AR but not the A_{2A}AR or that A_{2A}AR signaling is not coupled to osteogenic pathways. This idea is supported by reduced bone volume in A_{2B}AR deficient mice (data not shown) and previous studies that demonstrated a tight relationship between CD73 and the A_{2B}AR in endothelial and epithelial cell function (Strohmeier et al., 1997; Lennon et al., 1998; Eltzschig et al., 2003; Eckle et al., 2007; Takedachi et al., 2008). Although the mechanism by which CD73-generated adenosine activates the A_{2B}AR is not known yet, we speculate that the proximity between the A_{2B}AR and CD73 on microdomains of the plasma membrane may lead to efficient activation of the A_{2B}AR by CD73-generated adenosine.

In conclusion, we propose that endogenous adenosine generated by CD73 promotes osteoblast differentiation via A_{2B}AR signaling. The A_{2B}AR is a seven-transmembrane—spanning G protein—coupled receptor that is coupled to Gs and uses cAMP as a second messenger. It has been reported that cAMP promotes osteoblast function and the anabolic action of bone formation by enhancement of bone morphogenetic protein signaling (Nakao et al., 2009). Experiments are now

ongoing to further define the role of the A_{2B}AR in osteoblast differentiation. Together with our findings in this study, such information may lead to the development of new anabolic therapeutic targets for bone diseases.

Acknowledgments

MT is a research fellow of the Japan Society for the Promotion of Science. LFT holds the Putnam City Schools Distinguished Chair in Cancer Research. The authors thank Stephanie McGee, Patrick Marble, and Emiko Maeda for excellent technical assistance.

Literature Cited

Alatalo S, Peng Z, Janckila A, Kaija H, Vihko P, Vaananen H, Halleen J. 2003. A novel immunoassay for the determination of tartrate-resistant acid phosphatase 5b from rat serum. J Bone Miner Res 18:134–139.

Baron R, Rawadi G, Roman-Roman S. 2006. Wnt signaling: A key regulator of bone mass. Curr Top Dev Biol 76:103–127.

Beck GR. 2003. Inorganic phosphate as a signaling molecule in osteoblast differentiation. J Cell Biochem 90:234–243.

Blackburn M, Vance C, Morschl E, Wilson C. 2009. Adenosine receptors and inflammation. Handb Exp Pharmacol 193:215–269.

Buckley K, Golding S, Rice J, Dillon J, Gallagher J. 2003. Release and interconversion of P2 receptor agonists by human osteoblast-like cells. FASEB J 17:1401–1410.

Costa M, Barbosa A, Neto E, Sá-E-Sousa A, Freitas R, Neves J, Magalhães-Cardoso T, Ferreirinha F, Correia-de-Sá P. 2010. On the role of subtype selective adenosine receptor agonists during proliferation and osteogenic differentiation of human primary bone marrow stromal cells. J Cell Physiol 226:1353–1366.

Costa MA, Barbosa A, Neto E, Sá-e-Sousa A, Freitas R, Neves JM, Magalhães-Cardoso T, Ferreirinha F, Correia-de-Sá P. 2011. On the role of subtype selective adenosine receptor agonists during proliferation and osteogenic differentiation of human primary bone marrow stromal cells. J Cell Physiol 226:1353–1366.

Eckle T, Krahn T, Grenz A, Köhler D, Mittelbronn M, Ledent C, Jacobson M, Osswald H, Thompson L, Unertl K, Eltzschig H. 2007. Cardioprotection by ecto-5′-nucleotidase (CD73) and A2B adenosine receptors. Circulation 115:1581–1590.

Eltzschig H, Ibla J, Furuta G, Leonard M, Jacobson K, Enjyoji K, Robson S, Colgan S. 2003. Coordinated adenine nucleotide phosphohydrolysis and nucleoside signaling in posthypoxic endothelium: Role of ectonucleotidases and adenosine A2B receptors. J Exp Med 198:783–796.

Evans B, Elford C, Pexa A, Francis K, Hughes A, Deussen A, Ham J. 2006. Human osteoblast precursors produce extracellular adenosine, which modulates their secretion of IL-6 and osteoprotegerin. J Bone Miner Res 21:228–236.

Fatokun A, Stone T, Smith R. 2006. Hydrogen peroxide-induced oxidative stress in MC3T3-E1 cells: The effects of glutamate and protection by purines. Bone 39: 542–551.

Garnero P, Ferreras M, Karsdal M, Nicamhlaoibh R, Risteli J, Borel O, Qvist P, Delmas P, Foged N, Delaissé J. 2003. The type I collagen fragments ICTP and CTX reveal distinct enzymatic pathways of bone collagen degradation. J Bone Miner Res 18: 859–867.

Grol MW, Panupinthu N, Korcok J, Sims SM, Dixon SJ. 2009. Expression, signaling, and function of P2X7 receptors in bone. Purinergic Signal 5:205–221.

Haskó G, Linden J, Cronstein B, Pacher P. 2008. Adenosine receptors: Therapeutic aspects for inflammatory and immune diseases. Nat Rev Drug Discov 7:759–770.

Hauschka P, Lian J, Cole D, Gundberg C. 1989. Osteocalcin and matrix Gla protein: Vitamin K-dependent proteins in bone. Physiol Rev 69:990–1047.

Hsiao E, Boudignon B, Chang W, Bencsik M, Peng J, Nguyen T, Manalac C, Halloran B, Conklin B, Nissenson R. 2008. Osteoblast expression of an engineered Gs-coupled receptor dramatically increases bone mass. Proc Natl Acad Sci USA 105:1209–1214.

Kalsi K, Lawson C, Dominguez M, Taylor P, Yacoub M, Smolenski R. 2002. Regulation of ecto-5′-nucleotidase by TNF-alpha in human endothelial cells. Mol Cell Biochem 232:113–119.

Kara F, Doty S, Boskey A, Goldring S, Zaidi M, Fredholm B, Cronstein B. 2010a. Adenosine A(1) receptors regulate bone resorption in mice: Adenosine A(1) receptor blockade or deletion increases bone density and prevents ovariectomy-induced bone loss in adenosine A(1) receptor-knockout mice. Arthritis Rheum 62:534–541.

Kara FM, Chitu V, Sloane J, Axelrod M, Fredholm BB, Stanley ER, Cronstein BN. 2010b. Adenosine A1 receptors (A1Rs) play a critical role in osteoclast formation and function. FASEB J 24:2325–2333.

Katebi M, Soleimani M, Cronstein BN. 2009. Adenosine A2A receptors play an active role in mouse bone marrow-derived mesenchymal stem cell development. J Leukoc Biol 85:438–444.

Lennon P, Taylor C, Stahl G, Colgan S. 1998. Neutrophil-derived 5′-adenosine monophosphate promotes endothelial barrier function via CD73-mediated conversion to adenosine and endothelial A2B receptor activation. J Exp Med 188:1433–1443.

Nakao Y, Koike T, Ohta Y, Manaka T, Imai Y, Takaoka K. 2009. Parathyroid hormone enhances bone morphogenetic protein activity by increasing intracellular 3′, 5′-cyclic adenosine monophosphate accumulation in osteoblastic MC3T3-E1 cells. Bone 44:872–877.

Niemelä J, Henttinen T, Yegutkin G, Airas L, Kujari A, Rajala P, Jalkanen S. 2004. IFN-alpha induced adenosine production on the endothelium: A mechanism mediated by CD73 (ecto-5′-nucleotidase) up-regulation. J Immunol 172:1646–1653.

Orriss IR, Burnstock G, Arnett TR. 2010. Purinergic signalling and bone remodelling. Curr Opin Pharmacol 10:322–330.

Piters E, Boudin E, Van Hul W. 2008. Wnt signaling: A win for bone. Arch Biochem Biophys 473:112–116.

Ralevic V, Burnstock G. 1998. Receptors for purines and pyrimidines. Pharmacol Rev 50:413–492.

Resta R, Hooker S, Laurent A, Shuck J, Misumi Y, Ikehara Y, Koretzky G, Thompson L. 1994. Glycosyl phosphatidylinositol membrane anchor is not required for T cell activation through CD73. J Immunol 153:1046–1053.

Romanello M, Pani B, Bicego M, D'Andrea P. 2001. Mechanically induced ATP release from human osteoblastic cells. Biochem Biophys Res Commun 289:1275–1281.

Sakamoto A, Chen M, Nakamura T, Xie T, Karsenty G, Weinstein L. 2005. Deficiency of the G-protein alpha-subunit G(s)alpha in osteoblasts leads to differential effects on trabecular and cortical bone. J Biol Chem 280:21369–21375.

Shimegi S. 1998. Mitogenic action of adenosine on osteoblast-like cells, MC3T3-E1. Calcif Tissue Int 62:418–425.

Spychala J, Kitajewski J. 2004. Wnt and beta-catenin signaling target the expression of ecto-5′-nucleotidase and increase extracellular adenosine generation. Exp Cell Res 296:99–108.

Strohmeier G, Lencer W, Patapoff T, Thompson L, Carlson S, Moe S, Carnes D, Mrsny R, Madara J. 1997. Surface expression, polarization, and functional significance of CD73 in human intestinal epithelia. J Clin Invest 99:2588–2601.

Synnestvedt K, Furuta G, Comerford K, Louis N, Karhausen J, Eltzschig H, Hansen K, Thompson L, Colgan S. 2002. Ecto-5′-nucleotidase (CD73) regulation by hypoxia-inducible factor-1 mediates permeability changes in intestinal epithelia. J Clin Invest 110:993–1002.

Takedachi M, Qu D, Ebisuno Y, Oohara H, Joachims M, McGee S, Maeda E, McEver R, Tanaka T, Miyasaka M, Murakami S, Krahn T, Blackburn M, Thompson L. 2008. CD73-generated adenosine restricts lymphocyte migration into draining lymph nodes. J Immunol 180:6288–6296.

Thompson L, Eltzschig H, Ibla J, Van De Wiele C, Resta R, Morote-Garcia J, Colgan S. 2004. Crucial role for ecto-5′-nucleotidase (CD73) in vascular leakage during hypoxia. J Exp Med 200:1395–1405.

Thomson L, Ruedi J, Glass A, Moldenhauer G, Moller P, Low M, Klemens M, Massaia M, Lucas A. 1990. Production and characterization of monoclonal antibodies to the glycosyl phosphatidylinositol-anchored lymphocyte differentiation antigen ecto-5′-nucleotidase (CD73). Tissue Antigens 35:9–19.

Van De Wiele CJ, Vaughn JG, Blackburn MR, Ledent CA, Jacobson M, Jiang H, Thompson LF. 2002. Adenosine kinase inhibition promotes survival of fetal adenosine deaminase-deficient thymocytes by blocking dATP accumulation. J Clin Invest 110:395–402.

Volmer J, Thompson L, Blackburn M. 2006. Ecto-5′-nucleotidase (CD73)-mediated adenosine production is tissue protective in a model of bleomycin-induced lung injury. J Immunol 176:4449–4458.

Wan C, Gilbert S, Wang Y, Cao X, Shen X, Ramaswamy G, Jacobsen K, Alaql Z, Eberhardt A, Gerstenfeld L, Einhorn T, Deng L, Clemens T. 2008. Activation of the hypoxia-inducible factor-1alpha pathway accelerates bone regeneration. Proc Natl Acad Sci USA 105:686–691.

Wang Y, Wan C, Deng L, Liu X, Cao X, Gilbert S, Bouxsein M, Faugere M, Guldberg R, Gerstenfeld L, Haase V, Johnson R, Schipani E, Clemens T. 2007. The hypoxia-inducible factor alpha pathway couples angiogenesis to osteogenesis during skeletal development. J Clin Invest 117:1616–1626.

Williams B, Insogna K. 2009. Where Wnts went: The exploding field of Lrp5 and Lrp6 signaling in bone. J Bone Miner Res 24:171–178.

Yamashita Y, Hooker SW, Jiang H, Laurent AB, Resta R, Khare K, Coe A, Kincade PW, Thompson LF. 1998. CD73 expression and fyn-dependent signaling on murine lymphocytes. Eur J Immunol 28:2981–2990.

Yegutkin G. 2008. Nucleotide- and nucleoside-converting ectoenzymes: Important modulators of purinergic signalling cascade. Biochim Biophys Acta 1783:673–694.

Journal of
PERIODONTAL RESEARCH

J Periodont Res 2012; 47: 263–271

JOURNAL OF PERIODONTAL RESEARCH
doi:10.1111/j.1600-0765.2011.01430.x

Effects of L-ascorbic acid 2-phosphate magnesium salt on the properties of human gingival fibroblasts

K. Tsutsumi[1], H. Fujikawa[1], T. Kajikawa[2], M. Takedachi[2], T. Yamamoto[1], S. Murakami[2]

[1]Oral Care Research Laboratories, Research and Development Headquarters, Lion Corporation, Tokyo, Japan and [2]Division of Oral Biology and Disease Control, Department of Periodontology, Osaka University Graduate School of Dentistry, Osaka, Japan

Tsutsumi K, Fujikawa H, Kajikawa T, Takedachi M, Yamamoto T, Murakami S. Effects of L-ascorbic acid 2-phosphate magnesium salt on the properties of human gingival fibroblasts. J Periodont Res 2012; 47: 263–271. © 2011 John Wiley & Sons A/S

Background and Objective: L-Ascorbic acid 2-phosphate magnesium salt (APM) is an L-ascorbic acid (AsA) derivative developed to improve AsA stability and display effective biochemical characteristics. This study aimed to investigate the effects of APM on the functions and properties of human gingival fibroblasts with respect to the prevention of periodontal disease in comparison with those of AsA.

Material and Methods: Human gingival fibroblasts were incubated in the presence or absence of APM or L-ascorbic acid sodium salt (AsANa). Intracellular AsA was analysed by HPLC. Collagen synthesis was measured by ELISA and real-time RT-PCR. Intracellular reactive oxygen species (ROS) induced by hydrogen peroxide (H_2O_2) were quantified using a fluorescence reagent, and cell damage was estimated with calcein acetoxymethyl ester. Furthermore, intracellular ROS induced by tumor necrosis factor-α (TNF-α) were quantified, and expression of TNF-α-induced interleukin-8 expression, which increases due to inflammatory reactions, was measured by ELISA and real-time RT-PCR.

Results: APM remarkably and continuously enhanced intracellular AsA and promoted type 1 collagen synthesis and mRNA expression. Furthermore, APM decreased cell damage through the suppression of H_2O_2-induced intracellular ROS and inhibited interleukin-8 production through the suppression of TNF-α-induced intracellular ROS. These effects of APM were superior to those of AsANa.

Conclusion: These results suggest that APM is more effective than AsANa in terms of intake, collagen synthesis, decreasing cell damage and inhibiting interleukin-8 expression in human gingival fibroblasts. This suggests that local application of APM can help to prevent periodontal disease.

Kota Tsutsumi, MSc, Oral Care Research Laboratories, Research and Development Headquarters, Lion Corporation, 1-3-7, Honjo, Sumida-ku, Tokyo 130-8644, Japan
Tel: +81 3 3621 6446
Fax: +81 3 3626 2896
e-mail: k-tutumi@lion.co.jp

Key words: collagen; human gingival fibroblast; L-ascorbic acid 2-phosphate magnesium salt; reactive oxygen species

Accepted for publication September 26, 2011

L-Ascorbic acid (AsA), better known as vitamin C, has various biochemical functions, such as collagen synthesis in skin fibroblasts (1,2), phagocytosis of polymorphonuclear leukocytes (3), differentiation of several mesenchymal cell types (4) and antioxidant scavenging of reactive oxygen species (ROS; 5). However, AsA is highly unstable in aerobic conditions (6,7), neutral pH (8) and in solution (9).

L-Ascorbic acid 2-phosphate magnesium salt (APM) is an AsA derivative developed to improve AsA

stability. APM is highly resistant to degradation into AsA, even at neutral pH (10), but displays numerous biochemical characteristics, such as easy degradation into AsA in the presence of phosphatase from living tissues. Enhancement of collagen production in keratocytes (11) and skin fibroblasts (12) by APM has been reported. Furthermore, Kobayashi *et al.* (13) have demonstrated that APM can protect against lipid peroxidation and inflammation in cutaneous tissue induced by ultraviolet B exposure. Collagen synthesis by APM and its antioxidant properties are especially attractive to the skincare field.

Interestingly, these two functions are also required in gingival tissues for preventing periodontal disease. Human gingival fibroblasts are the major constituents of gingival tissues and maintain their homeostasis by regulating collagen metabolism (14). However, collagen in gingiva is degraded by MMP produced by periodontal pathogens or various host cells in inflamed periodontal tissues (15). Moreover, it has been reported that ROS, which play a major role in the etiology of periodontal disease, are induced by respiratory bursts of neutrophils (5,16) or by the proinflammatory signaling pathway (17–19). Many studies have indicated that ROS induce direct tissue destruction, such as collagen degradation and cell damage (20,21), or stimulate proinflammatory processes (22–24).

Therefore, the promotion of collagen synthesis and suppression of ROS by APM could be expected to contribute to the integrity of gingival tissues and prevention of periodontal disease. The aim of this study was to investigate the effects of APM on intake, collagen synthesis, and antioxidant and anti-inflammatory properties of human gingival fibroblasts in comparison with those of AsA.

Material and methods

Reagents

L-Ascorbic acid sodium salt (AsANa) was obtained from Wako Pure Chemical Industries (Osaka, Japan). APM was obtained from Showa Denko Co., Ltd (Tokyo, Japan). Hydrogen peroxide (H_2O_2) was obtained from Merck KgaA (Darmstadt, Germany). Calcein acetoxymethyl ester (calcein-AM) was obtained from Invitrogen Corporation (Carlsbad, CA, USA). Tumor necrosis factor-α (TNF-α) was obtained from R&D Systems Inc. (Minneapolis, MN, USA).

Cell culture

The protocol was reviewed and approved by the Institutional Review Board of the Osaka University Graduate School of Dentistry, and informed consent was obtained from all subjects participating in the study. Two cell lines of human gingival fibroblasts (HGF 1 and HGF 2) were obtained from biopsies of healthy gingiva from healthy volunteers as previously described (25). Cells of another human gingival fibroblast cell line, Gin-1, were obtained from DS Pharma Biomedical Co., Ltd (Osaka, Japan). Human gingival fibroblasts were grown in Dulbecco's modified Eagle's medium (DMEM; GIBCO, Carlsbad, CA, USA) containing 10% fetal calf serum (FCS; SAFC Biosciences, Lenexa, KS, USA) and routinely passaged by trypsinization when nearly confluent. The HGF 1 cells were the main cell line evaluated in this study, and other cell lines exhibited similar tendencies to this cell line. The following experiments were performed after seeding the cells onto a culture plate (6.7×10^3 cells/cm^2) and pre-incubating them for 24 h in DMEM containing 10% FCS.

Content of AsA and APM in human gingival fibroblasts

Human gingival fibroblasts were incubated in 75 cm^2 flasks with 50 μM AsANa or APM in DMEM containing 1% FCS for 12–48 h. To determine whether APM was degraded into AsA by phosphatase present in FCS, APM was diluted in a medium containing heat-inactivated FCS at 56°C for 30 min in the APM (inactivated) group. Human gingival fibroblasts were washed three times with phosphate-buffered saline after incubation and collected in 0.1 mL of cold 5% metaphosphoric acid by scraping. The cell suspensions were sonicated and centrifuged at 10,000 *g* for 15 min at 4°C. The cell extract supernatants were maintained at −80°C until ready for HPLC analysis. In brief, the separation of AsA from the supernatants was achieved by isocratic elution from an Inertsil® ODS-3 column (4.6 mm × 250 mm, particle size 5 μm; GL Science, Tokyo, Japan), which was kept at 40°C, with 25 mM KH_2PO_4–H_3PO_4 buffer (pH 2.0) containing 20 μM EDTA and 25 mM tetrabutylammonium hydrogen sulfate at a flow rate of 0.8 mL/min. AsA was detected by an electrochemical detector (Eicom, Kyoto, Japan) adjusted to 550 mV, and APM was detected by a UV-Vis detector (Shimadzu, Kyoto, Japan) at 240 nm.

Cell proliferation

Cell proliferation was assessed by the trypan blue dye exclusion assay. Human gingival fibroblasts were incubated in a six-well plate with 50 μM AsANa or APM in DMEM containing 1% FCS for 12–72 h. The number of living cells was counted under microscopic observation after harvesting by trypsinization and staining with trypan blue (Invitrogen Corporation).

Collagen synthesis

Human gingival fibroblasts were incubated in a six-well plate with 50 μM AsANa or APM in DMEM containing 1% FCS for 3–72 h. Subsequently, the amount of type 1 collagen produced by human gingival fibroblasts in the culture medium supernatant was determined in each well using the Human Type 1 Collagen ELISA Kit (ACBio, Kanagawa, Japan) according to the manufacturer's instructions.

Extraction of RNA and real-time RT-PCR

Total RNA from human gingival fibroblasts was isolated using the RNeasy Mini Kit (QIAGEN K.K., Tokyo, Japan), and first-strand cDNA was synthesized using random primer

hexamers and M-MLV reverse transcriptase (Invitrogen Corporation). Real-time RT-PCR was performed using the Power PCR SYBR Master Mix (Applied Biosystems, Carlsbad, CA, USA) and gene-specific primers (Sigma-Aldrich Japan, K.K., Genosys Division, Ishikari, Japan) in a 7300 fast real-time RT-PCR system (Applied Biosystems) according to the manufacturer's instructions. Amplification conditions consisted of an initial denaturation at 95°C for 10 min, followed by 40 cycles of denaturation at 95°C for 15 s, and annealing and elongation at 60°C for 60 s. The primer sequences were as follows: glyceraldehyde-3-phosphate dehydrogenase (GAPDH), 5′-GCACCGTCAAGGCTGAGAAC-3′ (forward), 5′-ATGGTGGTGAAGACGCCAGT-3′ (reverse); type 1 collagen, 5′-CTGCTGGACGTCCTGGTGAA-3′ (forward), 5′-ACGCTGTCCAGCAATACCTTGAG-3′ (reverse); and interleukin-8 (IL-8), 5′-ACACTGCGCCAACACAGAAATTA-3′ (forward), 5′-TTTGCTTGAAGTTTCACTGGCATC-3′ (reverse). Relative expression was obtained after normalization with gene expression of GAPDH.

Intracellular ROS

Generation of intracellular ROS induced by H_2O_2 or TNF-α stimulation was evaluated using a ROS detection reagent, 5-(and-6)-chloromethyl-2′, 7′-dichlorodihydrofluorescein diacetate, acetyl ester (CM-H_2DCFDA; Molecular Probes, Carlsbad, CA, USA). In brief, this reagent is hydrolysed by intracellular esterases and is converted to the highly fluorescent derivative 5-(and-6)-chloromethyl-2′,7′-dichlorofluorescein through its reaction with intracellular ROS. The quantification of fluorescence intensity enabled us to measure intracellular ROS. Human gingival fibroblasts were incubated in a 24-well plate with 50 μM AsANa or APM in DMEM containing 1% FCS for 12–72 h. Incubated cells were exposed to 10 μM CM-H_2DCFDA in serum-free DMEM for 30 min and washed with phosphate-buffered saline to eliminate the extracellular reagent. Subsequently, the cells were stimulated by 1 mM H_2O_2 in serum-free DMEM for 0.5 h. The intracellular fluorescence intensity was detected at 485 nm excitation and 530 nm emission using a fluorescence plate reader. Intracellular ROS levels were calculated by integrating the area under the fluorescence intensity–time curve and converted to the relative value compared with that in the samples without H_2O_2 stimulation. Transmitted and fluorescent light images of the cells were observed, and the fluorescence intensity of each fluorescence image was quantified by an IN Cell Analyzer 1000 (GE Healthcare Japan, Tokyo, Japan) and converted to a relative value against the control. Likewise, evaluation of intracellular ROS after 8 h of stimulation by TNF-α was performed using the CM-H_2CDFDA reagent.

Cell viability assay

Cell viability was determined on the basis of the metabolism of calcein-AM, which produces a green fluorescence on reaction with intracellular esterase. Human gingival fibroblasts incubated for 24 h in the presence of AsANa or APM were exposed to 1 μM calcein-AM in Dulbecco's phosphate-buffered saline for 30 min after stimulation with 1 mM H_2O_2 for 0.5–2 h. Fluorescence intensity was detected using a fluorescence spectrometer, and cell viability (as a percentage) was calculated as follows: (fluorescence intensity of each group after H_2O_2 stimulation)/(fluorescence intensity without H_2O_2 stimulation) × 100.

Determination of IL-8 production

Human gingival fibroblasts were incubated in a 24-well plate with 50 μM AsANa or APM in DMEM containing 1% FCS for 24 h. The cells were stimulated with 1 nM TNF-α in DMEM containing 1% FCS. After stimulation for 8 h, total RNA was isolated from the cells, and IL-8 mRNA expression was measured. Finally, the culture medium supernatants were assayed for IL-8 using the Human IL-8 ELISA Kit (R&D Systems, Minneapolis, MN, USA) according to the manufacturer's instructions.

Statistical analysis

ANOVA was used to compare groups, and the homogeneity of variance was confirmed by Bartlett's test. Tukey's multiple comparison test was used to determine differences among the three groups (control, AsANa and APM) with respect to cell proliferation, collagen synthesis, intracellular ROS, cell viability and IL-8 production. Unpaired student's *t*-test or the Aspin–Welch test was used to evaluate the changes in intracellular ROS and the amount of IL-8 produced in response to H_2O_2 or TNF-α stimulation.

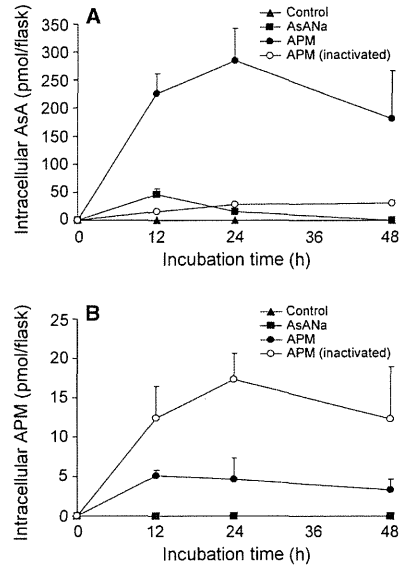

Fig. 1. The intracellular accumulation of L-ascorbic acid (AsA) and L-ascorbic acid 2-phosphate magnesium salt (APM) in human gingival fibroblasts. Human gingival fibroblasts were incubated in the presence or absence (control) of 50 μM of the sodium salt of AsA (AsANa) or APM in Dulbecco's modified Eagle's medium (DMEM) containing 1% fetal calf serum (FCS). Dulbecco's modified Eagle's medium containing 1% heat-inactivated FCS was used in the APM (inactivated) group. After incubation for 12–48 h, cell suspensions collected in 5% metaphosphoric acid were sonicated and centrifuged. The amount of intracellular AsA and APM in the supernatants was determined by HPLC. (A) AsA was detected by an electrochemical detector. (B) APM was detected by an UV-Vis detector. The results represent the means ± SD of three independent experiments.

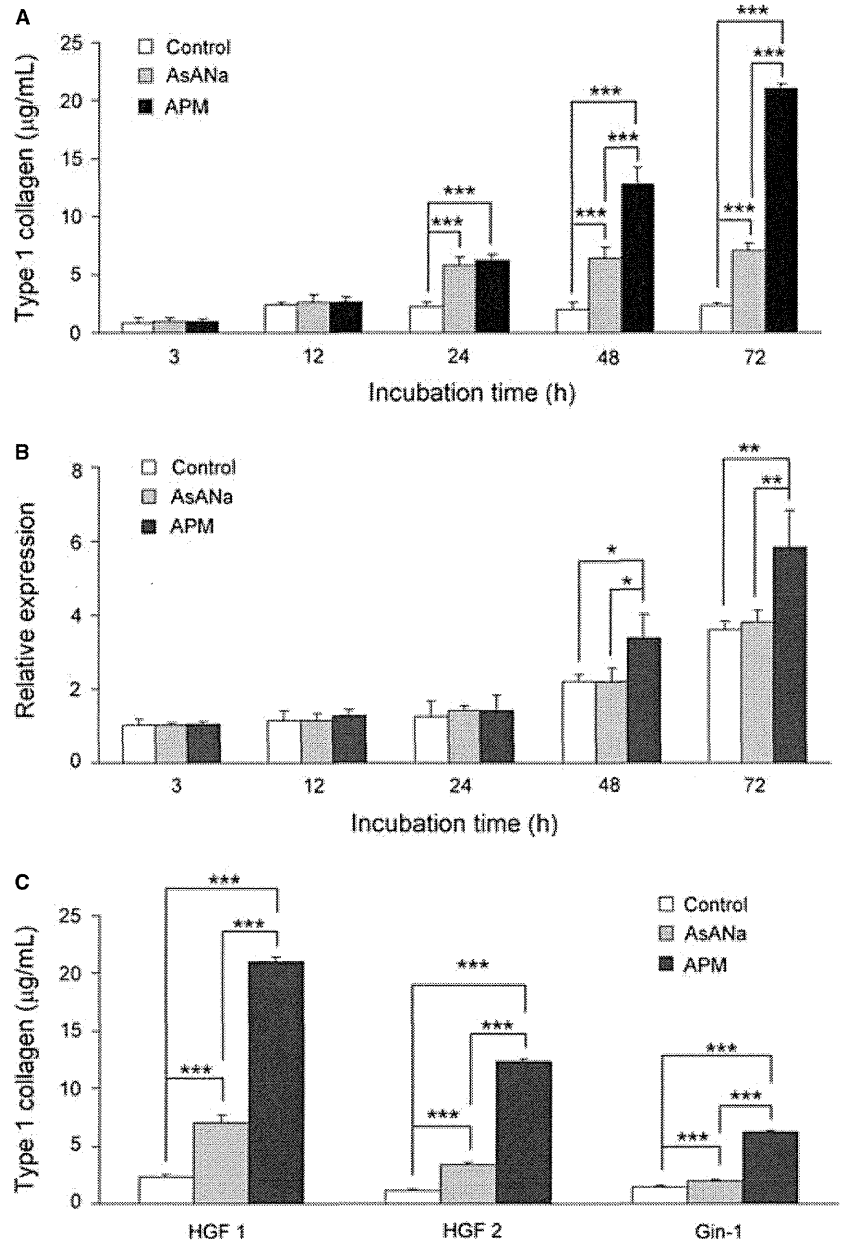

Fig. 2. Effects of AsANa and APM on collagen synthesis in human gingival fibroblasts. Human gingival fibroblasts were incubated in the presence or absence (control) of 50 μM AsANa or APM in DMEM containing 1% FCS for 12–72 h. (A) Cell culture supernatants of HGF 1 cells were measured using an ELISA kit. The results are shown as the means + SD (n = 5) of three independent experiments. (B) Type 1 collagen mRNA expression in HGF 1 cells was measured by real-time RT-PCR as described in the Material and methods section. The results are shown as the means + SD (n = 4) of three independent experiments. (C) After incubation for 72 h, the cell culture supernatants of HGF 1, HGF 2 and Gin-1 cells were measured using an ELISA kit. The results are shown as the means + SD (n = 5) of three independent experiments. *p < 0.05, **p < 0.01 and ***p < 0.001 by Tukey's test.

Results

The amount of intracellular AsA was remarkably enhanced by APM

To clarify differences in intake of AsA by human gingival fibroblasts between AsANa and APM groups, we quantified the amount of AsA and APM in the supernatant derived from crushed cells. The APM group showed a remarkably enhanced level of intracellular AsA (> 200 pmol per flask) at 12 h, and this level was maintained up to 48 h; although levels were within 30 pmol in the APM (inactivated) group in which phosphatase in FCS was inactivated (Fig. 1A). Conversely, intracellular AsA in the AsANa group disappeared at 48 h, although a peak value of 50 pmol was observed at 12 h. There was no intracellular AsA detected in the control group. The

amounts of intracellular APM in the APM and APM (inactivated) groups were approximately 5 and 15 pmol, respectively, up to 48 h (Fig. 1B).

APM promoted type 1 collagen synthesis and mRNA expression in a time-dependent manner

To investigate the effects of AsANa and APM on collagen synthesis in human gingival fibroblasts, we measured the amount of type 1 collagen synthesized by HGF 1 cells in the supernatant of the culture medium. No difference in collagen synthesis was observed among the three groups until 12 h of incubation, but the AsANa and APM groups showed a significant increase compared with the control group after 24 h (Fig. 2A). Collagen synthesis continued in the APM group and accelerated after 48 h, with a twofold higher level than that in the AsANa group at 48 h ($p < 0.001$) and a threefold higher level at 72 h ($p < 0.001$). To elucidate the cause of this acceleration, we evaluated type 1 collagen mRNA expression. The APM group showed significantly higher type 1 collagen mRNA expression at 48 ($p < 0.05$) and 72 h ($p < 0.01$) than that observed in the control and AsANa groups, whereas type 1 collagen mRNA expression in the AsANa group did not differ from that in the control group (Fig. 2B). This acceleration of collagen synthesis was also observed in HGF 2 and Gin-1 cells (Fig. 2C). However, no significant difference in the proliferation of HGF 1 cells was observed among the three groups at any incubation time point.

APM decreased cell damage by suppressing intracellular ROS produced by H_2O_2 stimulation

We evaluated intracellular ROS produced by H_2O_2 stimulation to clarify the antioxidative properties of AsANa and APM. Intracellular ROS levels in the control group increased more than twofold due to H_2O_2 stimulation at all incubation times ($p < 0.001$). The intracellular ROS scavenging activity levels as a percentage of those of the H_2O_2 alone group were 35 (12 h; $p < 0.01$), 38 (24 h; $p < 0.001$), 35 (48 h; $p < 0.001$) and 16% (72 h; $p < 0.05$) in the APM group and 23 (12 h; $p < 0.05$), 18 (24 h; $p < 0.01$), −3 (48 h; not significant) and −10% (72 h; not significant) in the AsANa group (Fig. 3A). The APM group showed significant suppression of intracellular ROS production up to 72 h, whereas in the AsANa group, the suppressive effect on ROS production disappeared at 48 h. Figure 4 illustrates the cell images produced by transmitted or fluorescent light and quantification of fluorescence images when the cells were incubated for 24 h followed by H_2O_2 stimulation. The strength of the yellowish-green intracellular fluorescence, which corresponded to intracellular ROS levels, in the APM group was remarkably reduced compared with that in the H_2O_2 alone and AsANa groups. This was consistent with the findings in Fig. 3A. We also measured cell viability to clarify whether cell damage was influenced by this ROS suppression. In all groups, cell damage appeared 1 h

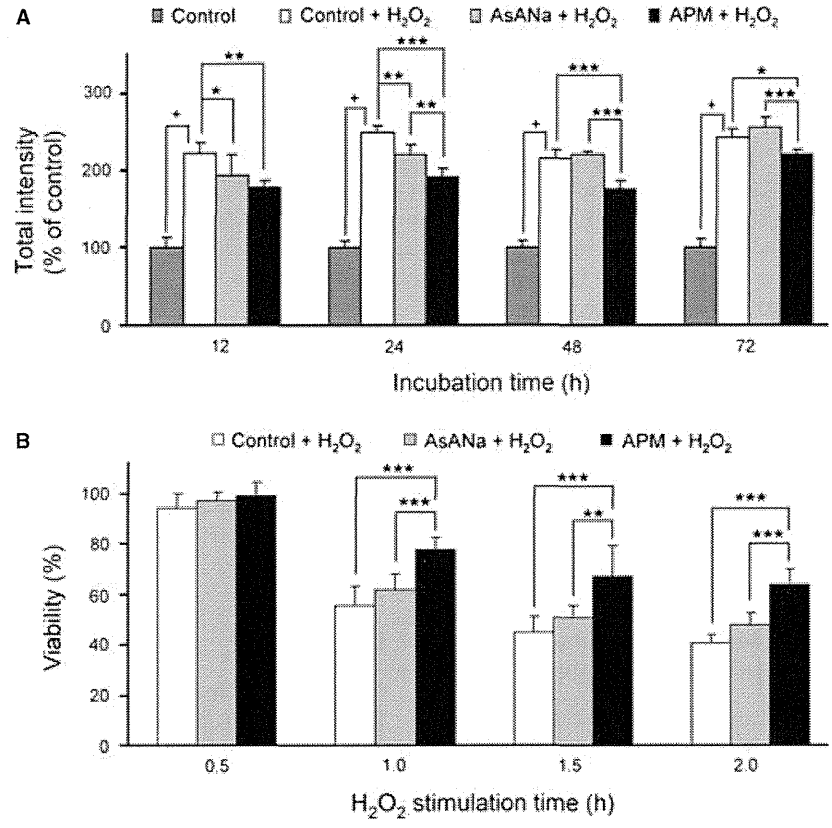

Fig. 3. Effects of APM and AsANa on hydrogen peroxide (H_2O_2)-induced intracellular reactive oxygen species (ROS) generation and cell damage in human gingival fibroblasts. Human gingival fibroblasts were incubated in the presence or absence (control) of 50 μM AsANa or APM in DMEM containing 1% FCS. (A) After incubation for 12–72 h, the cells were incubated for 30 min in serum-free DMEM containing 10 μM 5-(and-6)-chloromethyl-2′,7′-dichlorodihydrofluorescein diacetate, acetyl ester (CM-H_2DCFDA) and transferred to 1 mM H_2O_2 in serum-free DMEM. The ROS levels were immediately detected using a microplate fluorometer for 30 min. The results are shown as the means + SD ($n = 6$) of three independent experiments. $*p < 0.05$, $**p < 0.01$ and $***p < 0.001$ by Tukey's test; and $+p < 0.001$ by Unpaired student's *t*-test. (B) After a 24 h pretreatment for APM and AsANa, the cells were stimulated with 1 mM H_2O_2 for 0.5–2 h in serum-free DMEM and subsequently incubated for 30 min in Dulbeccos phosphate-buffered saline containing 1 μM calcein acetoxymethyl ester. The results are shown as the means + SD ($n = 6$) of three independent experiments. $*p < 0.05$, $**p < 0.01$ and $***p < 0.001$ by Tukey's test.

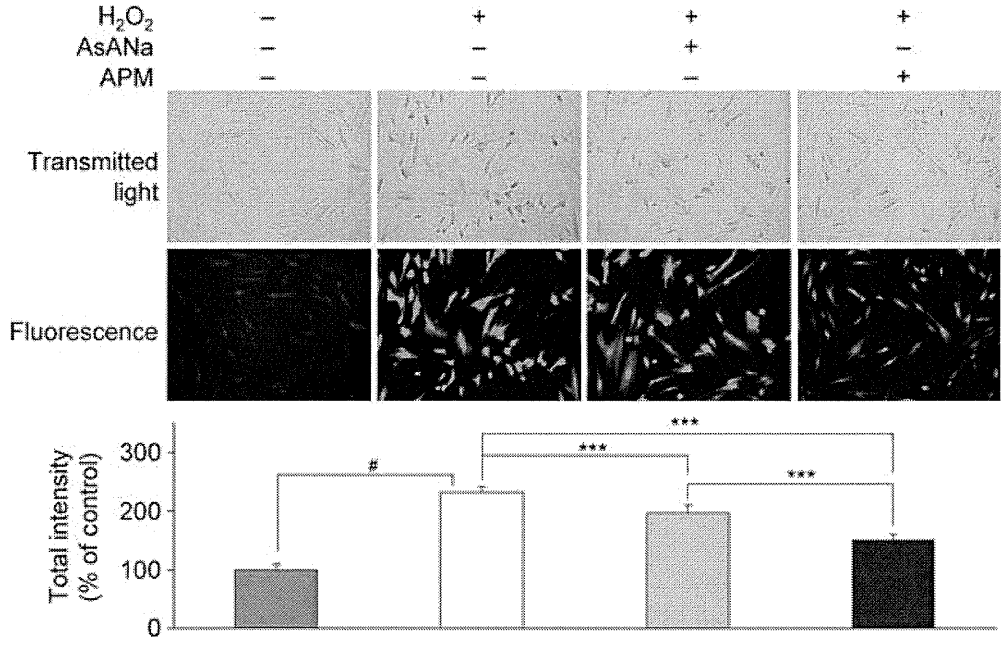

Fig. 4. Intracellular ROS scavenging activity of APM in human gingival fibroblasts. Human gingival fibroblasts were incubated in the presence or absence (control) of 50 μM AsANa or APM in DMEM containing 1% FCS for 24 h. After incubation, the cells were incubated for 30 min in serum-free DMEM containing 10 μM CM-H_2DCFDA and transferred to 1 mM H_2O_2 in serum-free DMEM for 30 min. Cell images were taken, and the fluorescence intensity of each image was quantified by the IN Cell Analyzer 1000. Cell images are representative of three independent experiments. Data are shown as the means + SD (n = 6) of three independent experiments. ***p < 0.001 by Tukey's test; and p < 0.01 by Aspin–Welch test.

after stimulation with H_2O_2, but cell damage in the APM group was significantly lower than that in the H_2O_2 alone (p < 0.001) and AsANa groups (p < 0.01; Fig. 3B).

APM inhibited IL-8 production by suppressing intracellular ROS through TNF-α stimulation

We investigated the effects of AsANa and APM on intracellular ROS and IL-8 production induced by TNF-α stimulation. The intracellular ROS level in the control group increased by approximately 40% due to TNF-α stimulation (p < 0.001). The APM group showed a 66% suppression of intracellular ROS levels (p < 0.01), but the AsANa group showed only an 8% suppression (not significant) in comparison to the values for the TNF-α alone group (Fig. 5A). In contrast, IL-8 production and mRNA expression increased remarkably after TNF-α stimulation. Interestingly, the APM group showed a 35% inhibition of IL-8 protein production (p < 0.001) and a 52% inhibition of IL-8 mRNA expression (p < 0.01) compared with the production in the TNF-α alone group (Fig. 5B and 5C). However, no significant differences were observed between the TNF-α alone and AsANa groups.

Discussion

APM is a stable AsA derivative, but the mechanism by which APM and AsA are taken up by human gingival fibroblasts has not yet been clarified. Interestingly, in our experiment quantifying intracellular AsA levels, the APM group showed an approximately 20-fold enhancement in the amount of AsA relative to that of the AsA group 24 h after incubation, and this effect was long lasting. We believe that enhancement and persistence of intracellular AsA in the APM group could be explained by the existence of AsA transporters and the gradual degradation of APM. Transport studies have revealed that mammalian cells are endowed with two types of transporters (SVCT 1 and SVCT 2) across their membrane (26), and various cells kinetically control the intake of AsA through these transporters by sodium or other cations (27,28). The transporters have a high specificity for AsA, but not for APM (26,29). The amount of intracellular intact APM in the APM group was lower than that of intracellular AsA, although we could detect intracellular APM. Therefore, we consider that intracellular AsA in the APM group was due to the intake of AsA after degradation. This possibility is supported by the result of the APM (inactivated) group wherein the amount of intracellular AsA was markedly decreased because of phosphatase inactivation in FCS. The lower amount of intracellular AsA in the APM (inactivated) group was probably due to active phosphatase on the cell membrane (30). Chepda *et al.* (30) also demonstrated that APM is gradually degraded to AsA to continuously supply AsA to the culture medium for many hours. This highly effective characteristic of APM has been demonstrated in other cells as well (31).

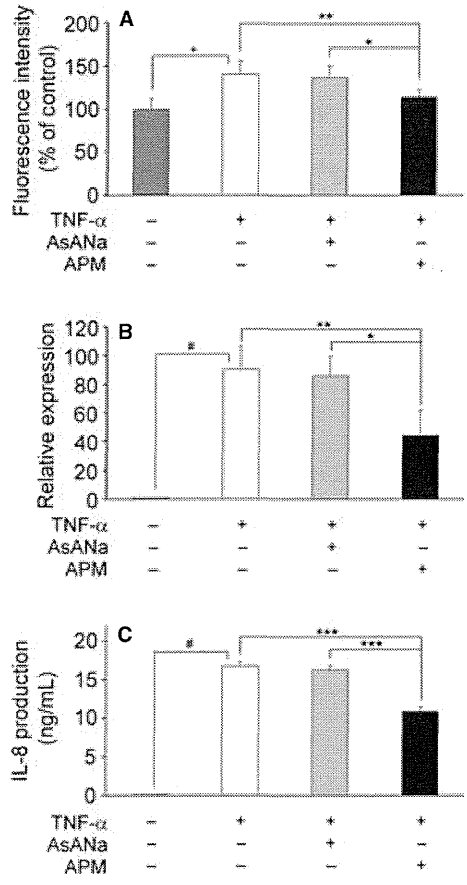

Fig. 5. Effects of APM and AsANa on tumor necrosis factor-α (TNF-α)-induced interleukin-8 (IL-8) production and intracellular ROS generation in human gingival fibroblasts. Human gingival fibroblasts were incubated in the presence or absence (control) of 50 μM AsANa or APM in DMEM containing 1% FCS for 24 h. After incubation, the cells were stimulated by 1 nM TNF-α for 8 h. (A) Intracellular ROS generation in human gingival fibroblasts was determined using CM-H_2DCFDA as described in the Material and methods section. Data are shown as the means + SD (n = 6) of three independent experiments. (B) Interleukin-8 mRNA expression was measured by real-time RT-PCR. The results are shown as the means + SD (n = 4) of three independent experiments. (C) Interleukin-8 in the culture medium was detected using an ELISA kit. The results are shown as the means + SD (n = 6) of three independent experiments. *p < 0.05, **p < 0.01 and ***p < 0.001 by Tukey's test; and p < 0.01 by Aspin–Welch test.

The main finding of this study was that type 1 collagen synthesis and intracellular ROS suppression were related to the amount of intracellular AsA. The type 1 collagen molecule consists of two α1 (1) and one α2 (1) polypeptide chains with a spiral form (32). Many studies have reported that AsA plays an important role as a cofactor for proline and lysine hydroxylase, which is required for the numerous hydrogen bonds needed to create the stable spiral form and produce a mature collagen structure (33). In the results shown in Fig. 3A, the promotion of collagen in the AsANa and APM groups at 24 h can be considered to be dependent on collagen maturation induced by increased intracellular AsA, because collagen mRNA expression did not change up to 24 h in the three groups, and collagen synthesis in the AsANa group after 48 h stopped at the same time that the intracellular AsA supply was exhausted. However, collagen synthesis after 48 h was accelerated in the APM group, contrary to the tendency of intracellular AsA levels to decrease. We would like to suggest that the increase in collagen mRNA expression strongly contributed to the acceleration in the APM group. Many studies have found that the type 1 collagen mRNA expression in various cells clearly increased in the presence of AsA, and this phenomenon has been attributed to mechanisms such as transcriptional control, a feedback effect produced by the procollagen polypeptide (34–36). In contrast, an increase in collagen mRNA expression in the AsANa group was not observed in this study. We speculate that this was because of the persistence of intracellular AsA at a high concentration. That is, in the present study, we only employed a single AsA treatment for 72 h, whereas daily AsA treatment was performed in most other studies.

Excess ROS levels have been implicated as the cause of various diseases, including periodontal disease (17). In periodontal lesions, neutrophils release excessive levels of superoxide, which is immediately converted to H_2O_2 (5). The H_2O_2 subsequently converts to hydroxyl radicals in the presence of metal ions in various tissues, and hydroxyl radicals induce the tissue dysfunction involved in cell damage (37). Previous studies have reported that H_2O_2 increases intracellular ROS and induces damage in various cells (17,21). In our study, the APM group showed remarkable suppression of intracellular ROS production and decreased cell damage after H_2O_2 stimulation, similar to the findings for other antioxidants (38,39). In addition, the effect was related to the amount of intracellular AsA that was capable of scavenging ROS (17). Thus, APM, which greatly enhanced intracellular AsA levels, can be expected to prevent tissue destruction caused by ROS in the progression of periodontal disease.

In this study, we investigated the anti-inflammatory properties of APM against the stimulatory effects of TNF-α, which is a major proinflammatory cytokine and induces intracellular ROS as signaling intermediates for proinflammatory cytokine production (17,24,40). On TNF-α stimulation, APM suppressed intracellular ROS production and inhibited IL-8 production in human gingival fibroblasts. These

effects appeared to be related to the intracellular AsA content. Many studies have reported that IL-8, which is an important factor in the chemotaxis of neutrophils (41), is induced by TNF-α stimulation in various cell types, including human gingival fibroblasts (42,43), and is detected in periodontal lesions (44,45). *N*-Acetyl-L-cysteine, a representative antioxidant, inhibited TNF-α-induced IL-8 production through the suppression of intracellular ROS (24). Furthermore, O'Hara *et al.* (46) found that *N*-acetyl-L-cysteine inactivated redox-sensitive transcription factors, such as nuclear factor-κB and activator protein-1. We speculate that the suppression of intracellular ROS production by APM may contribute to the inhibition of IL-8 production through the inactivation of nuclear factor-κB and activator protein-1 in human gingival fibroblasts.

Periodontal disease is an inflammatory disorder caused by periodontal pathogens. During the inflammatory process, MMP and ROS cause the destruction of periodontal tissues (5). Furthermore, continuous and excessive IL-8 secretion by human gingival fibroblasts induces unduly chemotactic activity of neutrophils and the initiation of chronic inflammatory responses, eventually leading to tissue destruction (41,44,45). Hence, the topical application of APM to periodontal lesions may promote gingival collagen synthesis and suppress excess ROS production through the enhancement of intracellular AsA levels, thereby blocking the destruction of periodontal tissue. A previous study reported that the phosphate derivatives of AsA penetrated through the epidermis of hairless mouse skin and were converted to AsA by phosphatase in the cell membrane (13). In addition, Shibayama *et al.* (47) demonstrated that the phosphate derivatives of AsA penetrated through a human epidermal skin model consisting of keratinocytes rather than AsA, after which they reached the site of the dermis mainly consisting of fibroblasts and collagen. Therefore, APM can be judged to penetrate through the gingival epithelia and reach the gingival fibroblasts, where it subsequently promotes gingival collagen synthesis, suppresses excess ROS production by enhancing intracellular AsA, and regulates the chronic inflammatory response through ROS suppression. Thus, the local application of APM can prevent periodontal disease.

Acknowledgements

We are grateful for the excellent technical support of Mitsuyoshi Iyama (Osaka University Graduate School of Dentistry) and the helpful discussion and suggestions of Shinichi Kataoka and Seiji Morishima (Lion Corporation).

References

1. Chan D, Lamande SR, Cole WG, Bateman JF. Regulation of procollagen synthesis and processing during ascorbate-induced extracellular matrix accumulation *in vitro*. *Biochem J* 1990;**269:** 175–181.
2. Pinnell SR. Regulation of collagen biosynthesis by ascorbic acid: a review. *Yale J Biol Med* 1985;**58:**553–559.
3. Thomas WR, Holt PG. Vitamin C and immunity: an assessment of the evidence. *Clin Exp Immunol*, 1978;**32:**370–379.
4. Duarte TL, Lunec J. Review: when is an antioxidant not an antioxidant? A review of novel actions and reactions of vitamin C *Free Radic Res* 2005;**39:**671–686.
5. Battino M, Bullon P, Wilson M, Newman H. Oxidative injury and inflammatory periodontal diseases: the challenge of antioxidants to free radicals and reactive oxygen species. *Crit Rev Oral Biol Med* 1999;**10:**458–476.
6. Austria R, Semenzato A, Bettero A. Stability of vitamin C derivatives in solution and topical formulations. *J Pharm Biomed Anal* 1997;**15:**795–801.
7. Segall AI, Moyano MA. Stability of vitamin C derivatives in topical formulations containing lipoic acid, vitamins A and E. *Int J Cosmet Sci* 2008;**30:**453–458.
8. Pappa-Louisi A, Pascalidou S. Optimal conditions for the simultaneous ion-pairing HPLC determination of L-ascorbic, dehydro-L-ascorbic, D-ascorbic, and uric acids with on-line ultraviolet absorbance and electrochemical detection. *Anal Biochem* 1998;**263:**176–182.
9. Kipp DE, Schwarz RI. Effectiveness of isoascorbate versus ascorbate as an inducer of collagen synthesis in primary avian tendon cells. *J Nutr* 1990;**120:**185–189.
10. Geesin JC, Gordon JS, Berg RA. Regulation of collagen synthesis in human dermal fibroblasts by the sodium and magnesium salts of ascorbyl-2-phosphate. *Skin Pharmacol* 1993;**6:**65–71.
11. Saika S, Uenoyama K, Hiroi K, Ooshima A. L-ascorbic acid 2-phosphate enhances the production of type I and type III collagen peptides in cultured rabbit keratocytes. *Ophthalmic Res* 1992;**24:**68–72.
12. Hata R, Senoo H. L-ascorbic acid 2-phosphate stimulates collagen accumulation, cell proliferation, and formation of a three-dimensional tissue-like substance by skin fibroblasts. *J Cell Physiol* 1989; **138:**8–16.
13. Kobayashi S, Takehana M, Itoh S, Ogata E. Protective effect of magnesium-L-ascorbyl-2 phosphate against skin damage induced by UVB irradiation. *Photochem Photobiol* 1996;**64:**224–228.
14. Mahanonda R, Pichyangkul S. Toll-like receptors and their role in periodontal health and disease. *Periodontol 2000* 2007;**43:** 41–55.
15. Preshaw PM. Host response modulation in periodontics. *Periodontol 2000* 2008;**48:** 92–110.
16. Miyasaki KT. The neutrophil: mechanisms of controlling periodontal bacteria. *J Periodontol* 1991;**62:**761–774.
17. Chapple IL, Matthews JB. The role of reactive oxygen and antioxidant species in periodontal tissue destruction. *Periodontol 2000* 2007;**43:**160–232.
18. Brigelius-Flohé R, Banning A, Kny M, Böl GF. Redox events in interleukin-1 signaling. *Arch Biochem Biophys* 2004;**423:** 66–73.
19. Chen X, Andresen BT, Hill M, Zhang J, Booth F, Zhang C. Role of reactive oxygen species in tumor necrosis factor-alpha induced endothelial dysfunction. *Curr Hypertens Rev* 2008;**4:**245–255.
20. Mukhopadhyay CK, Chatterjee IB. Free metal ion-independent oxidative damage of collagen. Protection by ascorbic acid. *J Biol Chem* 1994;**269:**30200–30205.
21. Waddington RJ, Moseley R, Embery G. Reactive oxygen species: a potential role in the pathogenesis of periodontal diseases. *Oral Dis* 2000;**6:**138–151.
22. Li G, Luna C, Liton PB, Navarro I, Epstein DL, Gonzalez P. Sustained stress response after oxidative stress in trabecular meshwork cells. *Mol Vis* 2007;**13:**2282–2288.
23. Hwang YS, Jeong M, Park JS *et al.* Interleukin-1beta stimulates IL-8 expression through MAP kinase and ROS signaling in human gastric carcinoma cells. *Oncogene* 2004;**23:**6603–6611.
24. Hashimoto S, Gon Y, Matsumoto K, Takeshita I, Horie T. N-acetylcysteine attenuates TNF-α-induced p38 MAP kinase activation and p38 MAP kinase-mediated IL-8 production by human

pulmonary vascular endothelial cells. *Br J Pharmacol* 2001;**132:**270–276.
25. Hashikawa T, Takedachi M, Terakura M *et al.* Activation of adenosine receptor on gingival fibroblasts. *J Dent Res* 2006;**85:** 739–744.
26. Savini I, Rossi A, Pierro C, Avigliano L, Catani MV. SVCT1 and SVCT2: key proteins for vitamin C uptake. *Amino Acids* 2008;**34:**347–355.
27. Godoy A, Ormazabal V, Moraga-Cid G *et al.* Mechanistic insights and functional determinants of the transport cycle of the ascorbic acid transporter SVCT2. Activation by sodium and absolute dependence on bivalent cations. *J Biol Chem* 2007;**282:** 615–624.
28. Wang Y, Mackenzie B, Tsukaguchi H, Weremowicz S, Morton CC, Hediger MA. Human vitamin C (L-ascorbic acid) transporter SVCT1. *Biochem Biophys Res Commun* 2000;**267:**488–494.
29. Tsukaguchi H, Tokui T, Mackenzie B *et al.* A family of mammalian Na^+-dependent L-ascorbic acid transporters. *Nature* 1999;**399:**70–75.
30. Chepda T, Cadau M, Girin P, Frey J, Chamson A. Monitoring of ascorbate at a constant rate in cell culture: effect on cell growth. *In Vitro* Cell Dev Biol Anim 2001;**37:**26–30.
31. Furumoto K, Inoue E, Nagao N, Hiyama E, Miwa N. Age-dependent telomere shortening is slowed down by enrichment of intracellular vitamin C via suppression of oxidative stress. *Life Sci* 1998;**63:**935–948.
32. Kurata S, Hata R. Epidermal growth factor inhibits transcription of type I collagen genes and production of type I collagen in cultured human skin fibroblasts in the presence and absence of L-ascorbic acid 2-phosphate, a long-acting vitamin C derivative. *J Biol Chem* 1991;**266:**9997–10003.
33. Peterkofsky B. Ascorbate requirement for hydroxylation and secretion of procollagen: relationship to inhibition of collagen synthesis in scurvy. *Am J Clin Nutr* 1991;**54:**1135S–1140S.
34. Vuust J, Sobel ME, Martin GR. Regulation of type I collagen synthesis. Total pro a 1(I) and pro a 2(I) mRNAs are maintained in a 2:1 ratio under varying rates of collagen synthesis. *Eur J Biochem* 1985; **151:**449–453.
35. Geesin JC, Darr D, Kaufman R, Murad S, Pinnell SR. Ascorbic acid specifically increases type I and type III procollagen messenger RNA levels in human skin fibroblast. *J Invest Dermatol* 1988;**90:**420–424.
36. Lyons BL, Schwarz RI. Ascorbate stimulation of PAT cells causes an increase in transcription rates and a decrease in degradation rates of procollagen mRNA. *Nucleic Acids Res* 1984;**12:**2569–2579.
37. Halliwell B, Clement MV, Long LH. Hydrogen peroxide in the human body. *FEBS Lett* 2000;**486:**10–13.
38. Kim SH, Kang KA, Zhang R *et al.* Protective effect of esculetin against oxidative stress-induced cell damage via scavenging reactive oxygen species. *Acta Pharmacol Sin* 2008;**29:**1319–1326.
39. Choi YJ, Jeong YJ, Lee YJ, Kwon HM, Kang YH. (−)Epigallocatechin gallate and quercetin enhance survival signaling in response to oxidant-induced human endothelial apoptosis. *J Nutr* 2005;**135:** 707–713.
40. Young CN, Koepke JI, Terlecky LJ, Borkin MS, Boyd Savoy L, Terlecky SR. Reactive oxygen species in tumor necrosis factor-a-activated primary human keratinocytes: implications for psoriasis and inflammatory skin disease. *J Invest Dermatol* 2008;**128:**2606–2614.
41. Okada H, Murakami S. Cytokine expression in periodontal health and disease. *Crit Rev Oral Biol Med* 1998;**9:**248–266.
42. Mahanonda R, Sa-Ard-Iam N, Montreekachon P *et al.* IL-8 and IDO expression by human gingival fibroblasts via TLRs. *J Immunol* 2007;**178:**1151–1157.
43. Takigawa M, Takashiba S, Myokai F *et al.* Cytokine-dependent synergistic regulation of interleukin-8 production from human gingival fibroblasts. *J Periodontol* 1994;**65:**1002–1007.
44. Wang PL, Ohura K, Fujii T *et al.* DNA microarray analysis of human gingival fibroblasts from healthy and inflammatory gingival tissues. *Biochem Biophys Res Commun* 2003;**305:**970–973.
45. Dongari-Bagtzoglou AI, Ebersole JL. Increased presence of interleukin-6 (IL-6) and IL-8 secreting fibroblast subpopulations in adult periodontitis. *J Periodontol* 1998;**69:**899–910.
46. O'Hara AM, Bhattacharyya A, Bai J *et al.* Tumor necrosis factor (TNF)-α-induced IL-8 expression in gastric epithelial cells: role of reactive oxygen species and AP endonuclease-1/redox factor (Ref)-1. *Cytokine* 2009;**46:**359–369.
47. Shibayama H, Hisama M, Matsuda S, Ohtsuki M. Permeation and metabolism of a novel ascorbic acid derivative, disodium isostearyl 2-O-L-ascorbyl phosphate, in human living skin equivalent models. *Skin Pharmacol Physiol* 2008;**21:** 235–243.

Journal of
PERIODONTAL RESEARCH

J Periodont Res 2012; 47: 55–61

JOURNAL OF PERIODONTAL RESEARCH
doi:10.1111/j.1600-0765.2011.01404.x

Irsogladine maleate regulates epithelial barrier function in tumor necrosis factor-α-stimulated human gingival epithelial cells

T. Fujita[1], H. Yumoto[2], H. Shiba[1], K. Ouhara[1], T. Miyagawa[1], T. Nagahara[1], S. Matsuda[1], H. Kawaguchi[1], T. Matsuo[2], S. Murakami[3], H. Kurihara[1]

[1]Department of Periodontal Medicine, Division of Frontier Medical Science, Hiroshima University Graduate School of Biomedical Sciences, Hiroshima, Japan, [2]Department of Conservative Dentistry, Institute of Health Biosciences, The University of Tokushima Graduate School, Tokushima, Japan and [3]Department of Periodontology, Division of Oral Biology and Disease Control, Osaka University Graduate School of Dentistry, Osaka, Japan

Fujita T, Yumoto H, Shiba H, Ouhara K, Miyagawa T, Nagahara T, Matsuda S, Kawaguchi H, Matsuo T, Murakami S, Kurihara H. Irsogladine maleate regulates epithelial barrier function in tumor necrosis factor-α-stimulated human gingival epithelial cells. J Periodont Res 2012; 47: 55–61. © 2011 John Wiley & Sons A/S

Background and Objective: As epithelial cells function as a mechanical barrier, the permeability of the gingival epithelial cell layer indicates a defensive capability against invasion by periodontal pathogens. We have reported the expression of claudin-1 and E-cadherin, key regulators of permeability, in the gingival junctional epithelium. Irsogladine maleate (IM) is a medication for gastric ulcers and also regulates *Aggregatibacter actinomycetemcomitans*-stimuated chemokine secretion and E-cadherin expression in gingival epithelium. In this study, we have further investigated the effects of IM on the barrier functions of gingival epithelial cells under inflammatory conditions.

Material and Methods: We examined the permeability, and the expression of claudin-1 and E-cadherin, in human gingival epithelial cells (HGECs) stimulated with tumor necrosis factor (TNF)-α, with or without IM.

Results: TNF-α increased the permeability of HGECs, and IM abolished the increase. TNF-α reduced the expression of E-cadherin in HGECs, and IM reversed the reduction. In addition, immunofluorescence staining showed that TNF-α disrupted claudin-1 expression in HGECs, and IM reversed this effect.

Conclusion: The results suggest that IM reverses the TNF-α-induced disruption of the gingival epithelial barrier by regulating E-cadherin and claudin-1.

Tsuyoshi Fujita, Department of Periodontal Medicine, Division of Frontier Medical Science, Hiroshima University Graduate School of Biomedical Sciences, 1-2-3, Kasumi, Minami-ku, Hiroshima 734-8553, Japan
Tel: +81 82 257 5663
Fax: +81 82 257 5664
e-mail: tfuji@hiroshima-u.ac.jp

Key words: claudin-1; E-cadherin; epithelial barrier; irsogladine maleate; tumor necrosis factor-α

Accepted for publication July 5, 2011

Periodontitis is an inflammatory condition caused by the colonization of periodontopathogenic bacteria, such as *Porphyromonas gingivalis* or *Aggregatibacter actinomycetemcomitans*, in the gingival sulcus. The gingival junctional epithelium is located at a strategically important interface at the bottom of the gingival sulcus and contributes actively to inflammatory processes because it represents the first line of defense against microbial attack (1–3). As epithelial cells function as a mechanical barrier (4,5), disruption of the gingival epithelial cell layer allows periodontopathogenic bacteria to invade periodontal tissue, leading to periodontal disease. Therefore, regulation of the barrier function may prevent bacterial invasion.

Although epithelial cells are generally interconnected by tight junctions, adherence junctions, desmosomes and gap junctions, previous studies have shown that the junctional epithelium is interconnected only by a few desmosomes, and occasionally by gap junctions, and has wide intercellular spaces (1,2). However, we recently found that claudin-1, a tight junction

structured protein, was expressed in the healthy junctional epithelium of Fischer 344 rats (6). A previous report showed that claudin-1-deficient mice died within 1 d of birth and exhibited severe defects in the permeability of the epidermis (7). Cells over-expressing claudin-1 showed increased transepithelial electrical resistance (8). Therefore, claudin-1 may play an important role in the barrier function of the junctional epithelium, in spite of the absence of tight junctions. E-cadherin, a key protein involved in the formation of desmosomes and adherens junctions, is known to regulate the permeability of epithelial cells (5,9). In the gastric mucosal epithelium, the disruption of E-cadherin seems to cause epithelial permeability to increase (10). Immunohistochemical staining has shown that E-cadherin is expressed in the healthy junctional epithelium of humans and rats (6,11) and that its level is decreased in diseased tissue (11,12). Therefore, E-cadherin plays an important role against bacterial invasion in the gingival junctional epithelium.

Irsogladine maleate (IM) is known to enhance gap junctional intercellular communication in cultured rabbit gastric epithelial and pancreatic cancer cells (13,14), and is used clinically as an anti-gastric ulcer agent. Our previous study showed that IM inhibits *A. actinomycetemcomitans*-induced inflammatory responses in the gingival epithelium by suppressing neutrophil migration *in vivo* and *in vitro* (12). In addition, IM rescued the *A. actinomycetemcomitans*-induced reduction in E-cadherin *in vivo* and *in vitro* (12). Furthermore, IM countered the reduction of gap junctional intercellular communication in cultures of human gingival epithelial cells (HGECs) stimulated with *A. actinomycetemcomitans* or interleukin (IL)-1β (15,16). As IM seems to regulate the inflammatory responses induced by bacterial attack and cytokine stimulation in the human gingival epithelium, it may be a candidate preventive medicine for periodontal disease.

Junctional epithelium, which is originally derived from the reduced enamel epithelium, may be replaced over time by a junctional epithelium formed by basal cells originating from the oral gingival epithelium (17). In fact, after gingivectomy, a new junctional epithelium is formed from the basal cells of the oral gingival epithelium (18–22). These findings show that the origin of the junctional epithelium is the same as that of the oral gingival epithelium, suggesting that the cultured gingival epithelial cells used in this study possess some characteristics of junctional epithelial cells.

Tumor necrosis factor-α (TNF-α) is a major inflammatory cytokine produced in response to *P. gingivalis* or *A. actinomycetemcomitans* infection (23). It has also been reported that TNF-α induces barrier dysfunction in many types of cells. In this study, to investigate the effect of IM on the gingival epithelial barrier, we examined permeability and junctional protein expression in HGECs following stimulation with TNF-α.

Material and methods

Preparation of cells

Healthy gingival tissues, which had been surgically dissected through the process of wisdom tooth extraction and which were to be discarded, were collected with the patients' informed consent. HGECs from three donors (two women, 24 and 27 years of age; and one man, 22 years of age) were isolated as previously described (15,16). Briefly, gingival tissues were treated with 0.025% trypsin and 0.01% EDTA overnight at 4°C, and divided into epithelial and connective tissues. The HGEC suspension was centrifuged at 120 *g* for 5 min, and the pellet was suspended in Humedia-KB2 medium (Kurabo, Osaka, Japan) containing 10 μg/mL of insulin, 5 μg/mL of transferrin, 10 μM 2-mercaptoethanol, 10 μM 2-aminoethanol, 10 μM sodium selenite, 50 μg/mL of bovine pituitary extract, 100 units/mL of penicillin and 100 μg/mL of streptomycin (Medium A). The cells were seeded in 60-mm plastic tissue-culture plates coated with type I collagen, and incubated in 5% CO_2/95% air at 37°C. When the cells reached subconfluence, they were harvested and subcultured.

A Simian virus-40 (SV40) antigen-immortalized gingival epithelial cell line, OBA-9, was kindly provided by Dr Shinya Murakami (Osaka University Graduate School of Dentistry, Osaka, Japan) and maintained in Medium A (24). OBA-9 cells were used for immunofluorescence staining.

RNA preparation and real-time PCR

Cultured HGECs were harvested at the fourth passage, seeded in 35-mm plastic tissue-culture plates coated with type I collagen and maintained in 2 mL of Medium A. Confluent HGECs were pretreated for 1 h with or without 1 μM IM (supplied by Nippon Shinyaku, Kyoto, Japan) and then exposed for 24 h to 50 ng/mL of TNF-α (R&D Systems, Minneapolis, MN, USA) in 2 mL of Humedia-KB2 medium containing 10 μg/mL of insulin, 5 μg/mL of transferrin, 10 μM 2-mercaptoethanol, 10 μM 2-aminoethanol, 10 μM sodium selenite, 100 units/mL of penicillin and 100 μg/mL of streptomycin (Medium B). Total RNA was extracted using ISOGEN (Wako Pure Chemical Industries, Osaka, Japan) and quantified by spectrometry at 260 and 280 nm. First-strand cDNA synthesis was performed with 1 μg of total RNA extract in a total volume of 20 μL (Roche, Tokyo, Japan). Real-time PCR was performed with a Lightcycler system using SYBR Green (Roche). The sense and antisense primers for human E-cadherin, claudin-1 and glyceraldehyde-3-phosphate dehydrogenase (*GAPDH*) mRNA are listed in Table 1.

Western blotting

To analyze the expression of claudin-1, E-cadherin and β-actin, HGECs were cultured as described above. Confluent HGECs, which had been pretreated for 1 h with or without 1 μM IM, were exposed to 50 ng/mL of TNF-α for 24 h in 2 mL of Medium B. The cells were lysed in 200 μL of sodium dodecyl sulfate (SDS) sample buffer (62.5 mM Tris–HCl, 2% SDS, 10% glycerol, 50 mM dithiothreitol and 0.01% Bromophenol Blue). The samples were resolved on a 10%

Table 1. Primers for the real-time PCR used in this study

Claudin-1
Sense: 5′-GCG CGA TAT TTC TTC TTG CAG G-3′
Antisense: 5′-TTCGTACCTGGCATT GACTGG-3′
E-cadherin
Sense: 5′-TTC TGC TGC TCT TGC TGT TTC-3′
Anti-sense: 5′-AGT CAAAGT CCT GGT CCT CTT-3′
GAPDH
Sense: 5′-AAC GTG TCA GTG GTG GAC CTG-3′
Antisense: 5′-AGT GGG TGT CGC TGT TGA AGT-3′

GAPDH, glyceraldehyde-3-phosphate dehydrogenase.

SDS-polyacrylamide gel by electrophoresis under nonreducing conditions and electrophoretically transferred onto membranes (Bio-Rad Laboratories, Hercules, CA, USA). The membranes were blocked for 1 h with 5% nonfat dried milk and reacted overnight with mouse anti-human E-cadherin IgG (R&D Systems), rabbit anti-claudin-1 IgG (Invitrogen, Carlsbad, CA, USA) and mouse anti-human β-actin IgG (Invitrogen). Then, the membrane was incubated with horseradish peroxidase (HRP)-conjugated sheep anti-rabbit or goat anti-mouse IgG (R&D Systems) in Tris-buffered saline for 1 h at room temperature. Immunodetection was performed according to the manual supplied with the ECL Plus western blotting detection reagents (GE Healthcare, Bucks., UK).

Immunofluorescence staining

Fourth-passage HGECs, or OBA-9 cells, were seeded on glass coverslips coated with type I collagen in 35-mm plastic tissue-culture plates, and maintained in 2 mL of Medium A. Confluent HGECs or OBA-9 cells, which had been pretreated for 1 h with or without 1 μM IM, were exposed to 50 ng/mL of TNF-α for 24 h in 2 mL of Medium B. After incubation, the cells on the coverslips were washed and immersed for 10 min in 3.5% formaldehyde and 0.2% Triton X-100 in phosphate-buffered saline. Blocking was performed by immersing the coverslips in Tris-buffered saline, containing 0.2% casein and 0.1% Triton X-100, for 30 min at 37°C. After blocking, the coverslips were washed twice with phosphate-buffered saline. For staining of claudin-1 or E-cadherin, HGECs or OBA-9 cells were labeled with rabbit anti-claudin-1 IgG or mouse anti-human E-cadherin IgG (Takara, Shiga, Japan), followed by Alexa Fluor 488-conjugated anti-rabbit or anti-mouse IgG. Fluorescence signals were detected using a Zeiss LSM 510 laser scanning confocal microscope (Zeiss Microimaging, Thornwood, NY, USA) or a fluorescence microscope, BZ-9000 (Keyence, Osaka, Japan). The immunofluorescence intensity was quantitatively measured.

Transepithelial electrical resistance

HGECs were seeded on cell-culture polyethylene terephthalate membrane inserts (ThinCerts, 0.4 μm pore size; Greiner Bio-One, Frickenhausen, Germany) placed in a 24-well tissue culture plate and maintained in 800 μL of Medium A. Confluent HGECs were pretreated for 1 h with or without 1 μM IM, and then exposed to 10, 50 or 100 ng/mL of TNF-α for 0, 12, 24, or 31 h in Medium B. The transepithelial electrical resistance (TER) of HGECs was measured using a Millicell-ERS (Millipore, Billerica, MA, USA).

Fluorescein–dextran conjugate transport assay

To examine cell permeability, we also used a fluorescein–dextran conjugate

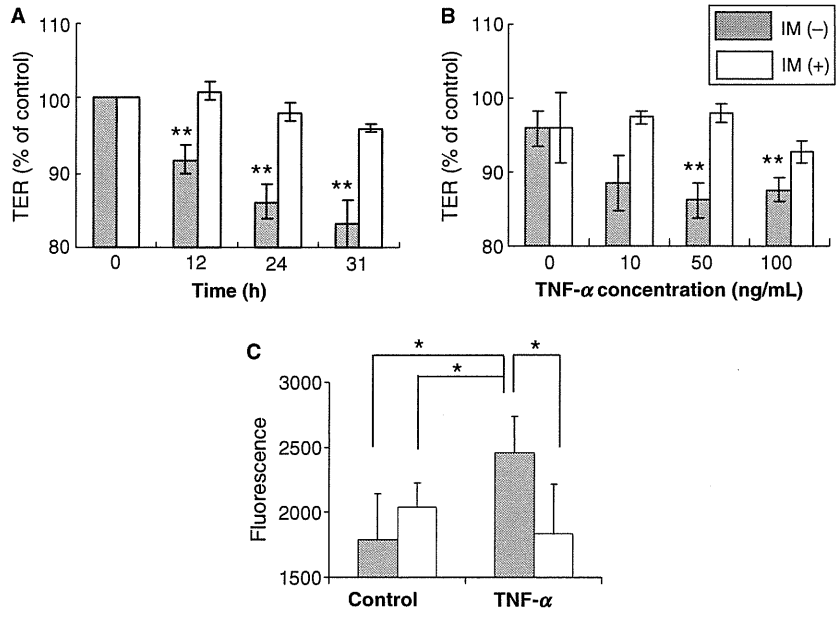

Fig. 1. Effect of irsogladine maleate (IM) on the permeability of the human gingival epithelial cell (HGEC) layer exposed to tumor necrosis factor-α (TNF-α). (A, B) Transepithelial electrical resistance (TER) of the HGEC layer. Confluent HGECs on the cell-culture polyethylene terephthalate membrane insert were pretreated for 1 h with or without 1 μM IM and then exposed to 50 ng/mL of TNF-α for the indicated times (A) or to 0–100 ng/mL of TNF-α for 24 h (B). The TER of HGECs was measured using a Millicell-ERS. **Significant difference from control (0 h) (Student's *t*-test, $p < 0.01$). (C) Fluorescein–dextran conjugate transport assay. Confluent HGECs on cell-culture polyethylene terephthalate membrane inserts were pretreated for 1 h with or without 1 μM IM and then exposed to 50 ng/mL of TNF-α for 24 h. Fluorescein–dextran conjugate was then added to the upper chamber to give a final concentration of 10 μg/mL. Four hours after the addition of fluorescein–dextran conjugate, the medium was collected from the lower chamber and the concentration was measured using a fluorescence microplate reader with excitation at 485 nm and emission at 535 nm. *Significant difference (Student's *t*-test, $p < 0.05$).

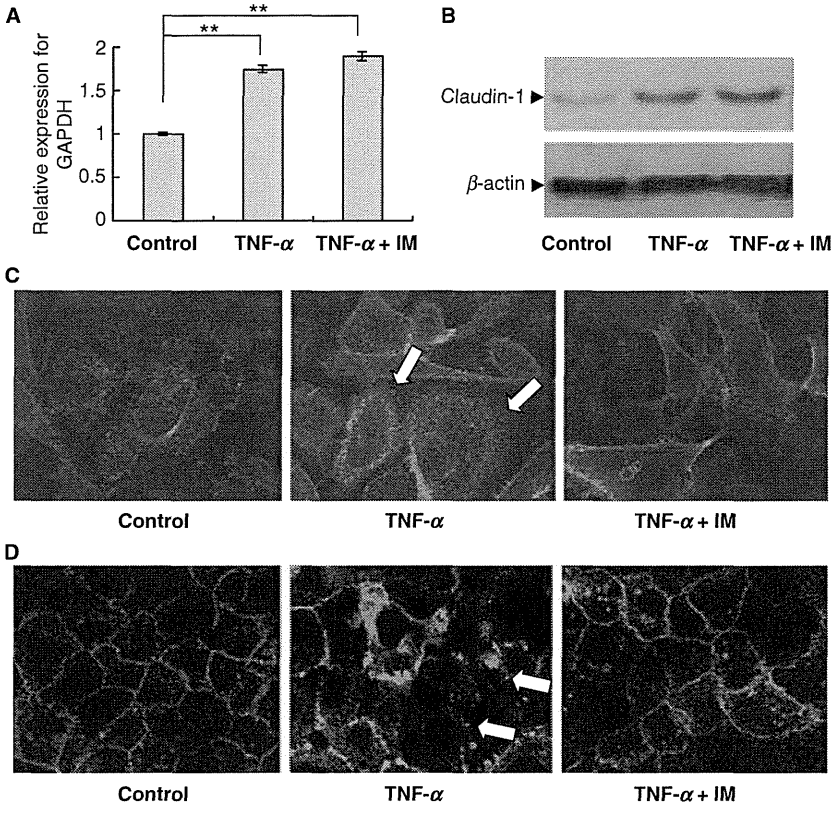

Fig. 2. Effect of irsogladine maleate (IM) on the expression of claudin-1 in human gingival epithelial cells (HGECs) and OBA-9 cells exposed to tumor necrosis factor-α (TNF-α). Confluent HGECs and OBA-9 cells were exposed to 50 ng/mL of TNF-α in the presence or absence of 1 μM IM for 24 h. (A) Claudin-1 mRNA in HGECs was analyzed using real-time PCR. Values are means ± standard deviation of three cultures. **Significant difference (*t*-test, $p < 0.01$). (B) Claudin-1 levels in HGECs were determined by western blotting. The bands are representative of three experiments. (C, D) Representative fluorescence images of the cellular distribution of claudin-1 in HGECs (C) or OBA-9 cells (D) was obtained using microscopy (×640 magnification). Arrows indicate the disruption of claudin-1 scattered in the cytoplasmic compartment. GAPDH, glyceraldehyde-3-phosphate dehydrogenase.

transport assay. HGECs were seeded on cell-culture polyethylene terephthalate membrane inserts, as described above. Confluent HGECs were pretreated for 1 h with or without 1 μM IM, and then exposed for 24 h to 50 ng/mL of TNF-α in Medium B. Fluorescein–dextran conjugate (molecular weight = 3000; Molecular Probes, Eugene, OR, USA) was added to the upper chamber to give a final concentration of 10 μg/mL. Four hours after the addition of fluorescein–dextran conjugate, the medium was collected from the lower chamber, and the fluorescence level was measured with excitation at 485 nm and emission at 535 nm using a fluorescence microplate reader (Twinkle LB 970; Berthold Technologies, Bad Wildbad, Germany).

Statistical analysis

Between-group comparisons were analyzed using the Student's *t*-test. Differences were considered significant when the probability value was < 5% ($p < 0.05$).

Results

IM inhibited the TNF-α-induced increase in the permeability of HGECs

At 50 ng/mL, TNF-α decreased the TER in HGECs, starting 12 h after exposure and continuing at a steady rate (Fig. 1A). In addition, treatment with 50 and 100 ng/mL of TNF-α for 24 h reduced the TER in HGECs (Fig. 1B). However, pretreatment with IM prevented the TNF-α-induced reduction (Fig. 1A and 1B). In addition, using the fluorescein–dextran conjugate transport assay, we confirmed the effect of IM on the permeability of HGECs stimulated by TNF-α. TNF-α increased the concentration of fluorescein–dextran conjugate in the lower chamber, and IM inhibited this increase (Fig. 1C).

E-cadherin and claudin-1 were present in HGECs and OBA-9 cells

Immunofluorescence staining showed junctional localization of claudin-1 and E-cadherin in the primary cultures of HGECs and in immortalized HGECs (OBA-9), and the immunofluorescence staining of OBA-9 cells was stronger than that of HGECs (Figs 2 and 3). Therefore, OBA-9 cells were also used to indicate the disruption of junctional proteins induced by TNF-α.

IM prevented the disruption of claudin-1 and E-cadherin induced by TNF-α in HGECs and OBA-9 cells

At 50 ng/mL, TNF-α increased the expression of claudin-1 at the mRNA and protein levels, and IM did not affect the increased levels of claudin-1 expression (Fig. 2A and 2B). However, immunofluorescence staining showed that 50 ng/mL of TNF-α affected the distribution of claudin-1 in HGECs and OBA-9 cells, and the disrupted claudin-1 proteins were scattered in the cytoplasmic compartment (Fig. 2C and 2D). In addition, IM reversed the TNF-α-induced disruption without changing the levels of mRNA and protein in HGECs and OBA-9 cells. TNF-α suppressed the expression of E-cadherin at the mRNA and protein levels, and IM prevented this decrease (Fig. 3A and 3B). Immunofluorescence staining also indicated that IM recovered the degradation of E-cadherin induced by TNF-α in HGECs and OBA-9 cells (Fig. 3C and 3D).

Discussion

In this study, we demonstrated, for the first time, that IM regulates gingival epithelial permeability by preventing the TNF-α-induced disruption of E-cadherin and claudin-1. At a cellular level, this result supports our previous finding that IM recovered the down-regulated expression of E-cadherin in inflammatory gingival tissue in an animal model.

In the present study, the addition of TNF-α to cultures of gingival epithelial cells increased cell permeability, consistent with previous reports in human airway epithelial cells (25), Caco-2 intestinal epithelial cells (26), human corneal epithelial cells (27) and human corneal endothelial cells (28). The involvement of cytokines in the breakdown of barrier integrity is recognized in many disorders, including pulmonary edema (29) and Crohn's disease (30). The increased permeability by cytokines gives the bacteria and their products the opportunity to enter the junctional epithelium. Therefore, the inhibition of enhancement of cell permeability by IM may protect gingival cells from bacterial invasion.

Although tight junctions, which generally contribute to the regulation of cell permeability, are considered not to exist in the gingival junctional epithelium, we previously found that claudin-1 is present in the gingival junctional epithelium (6). Therefore, we hypothesized that claudin-1 is involved in the permeability of the gingival epithelium in spite of the lack of tight junctions. Although TNF-α unexpectedly increased the expression of claudin-1 mRNA and protein, immunofluorescence staining showed that TNF-α disrupted claudin-1. Similarly, in the human colon carcinoma cell line HT-29/B6, TNF-α mediated claudin-1 internalization into intercellular vesicles while increasing expression levels (31). On the other hand, TNF-α down-regulated claudin-1 expression at the protein level in a rat parotid cell line and in human coronary artery endothelial cells (32,33). These different effects of TNF-α on claudin-1 expression might be a result of the source of cells or of the culture conditions. In addition, IM recovered the disruption of claudin-1 without affecting the increased expression levels. This result is supported by our

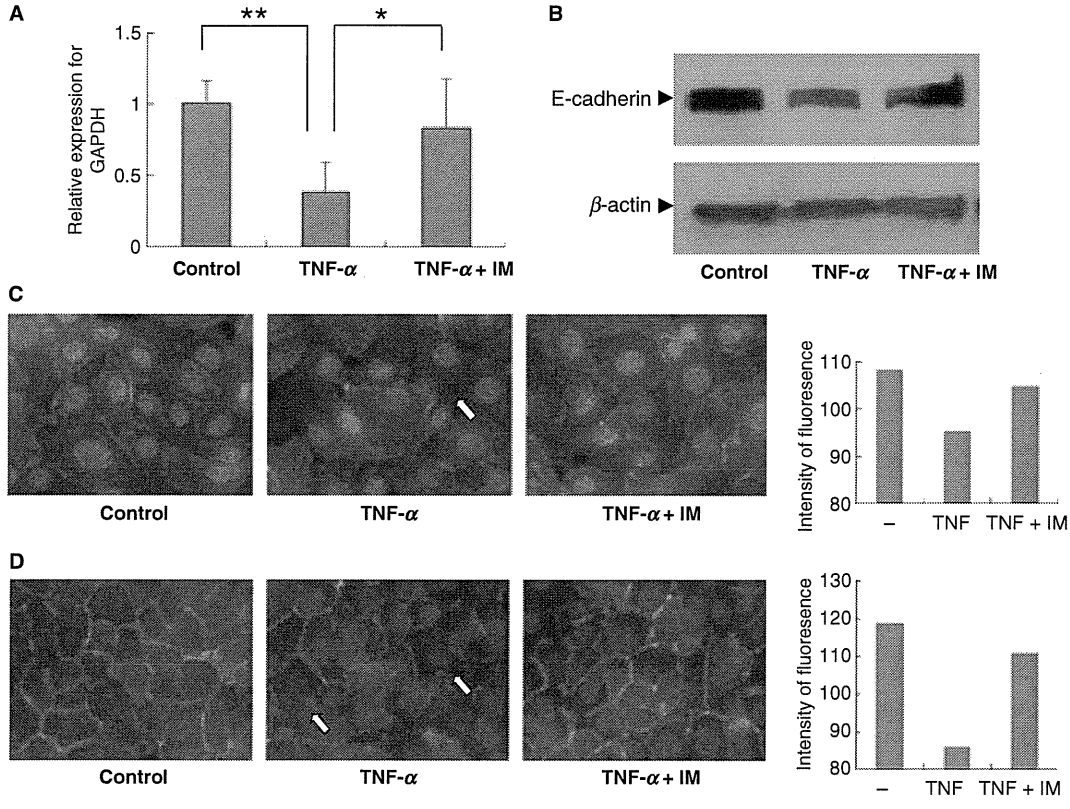

Fig. 3. Effect of irsogladine maleate (IM) on the expression of E-cadherin in human gingival epithelial cells (HGECs) and OBA-9 cells exposed to tumor necrosis factor-α (TNF-α). Confluent HGECs and OBA-9 cells were exposed to 50 ng/mL of TNF-α in the presence or absence of 1 μM IM for 24 h. (A) E-cadherin mRNA in HGECs was analyzed using real-time PCR. The mean value ± standard deviation of six cultures is shown. *Significant difference ($p < 0.05$); **Significant difference ($p < 0.01$) (both Student's *t*-test). (B) E-cadherin levels in HGECs were determined by western blotting. The bands are representative of three experiments. (C, D) Representative fluorescence images of the cellular distribution of E-cadherin in HGECs (C) or OBA-9 cells (D) were obtained using microscopy (×400 magnification). The immunofluorescence intensity was measured quantitatively by histogram function. Arrows indicate the degradation of E-cadherin. GAPDH, glyceraldehyde-3-phosphate dehydrogenase.

previous finding that IM did not affect the increased levels of ZO-1, a structural protein of tight junctions, induced by IL-1β in HGECs (34). These results may suggest that the total amount of tight junction structured proteins does not affect gingival epithelial cell permeability.

TNF-α suppressed and disrupted E-cadherin in HGECs, consistent with previous reports that TNF-α induces a significant decrease and disruption of E-cadherin in small airway epithelial cells, human bronchial epithelial cells and human nasal epithelial cells (35,36). However, in the present study, IM recovered the reduction of E-cadherin expression induced by TNF-α in HGECs. In addition, our previous report has shown that IM recovered *A. actinomycetemcomitans*-induced reduction of E-cadherin in rat gingival epithelium. As E-cadherin is a key protein in the formation of cell junctions in the gingival junctional epithelium, its recovery may result in enhancement of the epithelial barrier function.

Although further study is required, the previous and present data suggest the therapeutic efficiency of IM in the suppression of periodontal inflammation. IM has been used clinically as a medicament that protects the gastric mucosa. IM, by regulating the physical barrier in gingival epithelial cells, may be useful for the prevention of periodontal disease.

Acknowledgements

We thank the Nippon Shinyaku Co., Ltd. (Kyoto, Japan) for donating IM. We are grateful to Mr Tomoya Matsumoto (Keyence) for technical support. This study was supported in part by a Grant-in-aid for the Encouragement of Young Scientists (B) (no. 22792087) from the Japan Society for the Promotion of Science, Japan.

References

1. Shimono M, Ishikawa T, Enokiya Y *et al.* Biological characteristics of the junctional epithelium. *J Electron Microsc (Tokyo)* 2003;**52:**627–639.
2. Bosshardt DD, Lang NP. The junctional epithelium: from health to disease. *J Dent Res* 2005;**84:**9–20.
3. Schroeder HE, Listgarten MA. The junctional epithelium: from strength to defense. *J Dent Res* 2003;**82:**158–161.
4. Spring KR. Routes and mechanism of fluid transport by epithelia. *Annu Rev Physiol* 1998;**60:**105–119.
5. Niessen CM. Tight junctions/adherens junctions: basic structure and function. *J Invest Dermatol* 2007;**127:**2525–2532.
6. Fujita T, Hayashida K, Shiba H *et al.* The expressions of claudin-1 and E-cadherin in junctional epithelium. *J Periodontal Res* 2010;**45:**579–582.
7. Furuse M, Hata M, Furuse K *et al.* Claudin-based tight junctions are crucial for the mammalian epidermal barrier: a lesson from claudin-1-deficient mice. *J Cell Biol* 2002;**156:**1099–1111.
8. Inai T, Kobayashi J, Shibata Y. Claudin-1 contributes to the epithelial barrier function in MDCK cells. *Eur J Cell Biol* 1999;**78:**849–855.
9. Wheelock MJ, Jensen PJ. Regulation of keratinocyte intercellular junction organization and epidermal morphogenesis by E-cadherin. *J Cell Biol* 1992;**117:**415–425.
10. Wessler S, Backert S. Molecular mechanisms of epithelial-barrier disruption by *Helicobacter pylori*. *Trends Microbiol* 2008;**16:**397–405.
11. Ye P, Chapple CC, Kumar RK, Hunter N. Expression patterns of E-cadherin, involucrin, and connexin gap junction proteins in the lining epithelia of inflamed gingiva. *J Pathol* 2000;**192:**58–66.
12. Fujita T, Kishimoto A, Shiba H *et al.* Irsogladine maleate regulates neutrophil migration and E-cadherin expression in gingival epithelium stimulated by *Aggregatibacter actinomycetemcomitans*. *Biochem Pharmacol* 2010;**79:**1496–1505.
13. Kawasaki Y, Tsuchida A, Sasaki T *et al.* Irsogladine malate up-regulates gap junctional intercellular communication between pancreatic cancer cells via PKA pathway. *Pancreas* 2002;**25:**373–377.
14. Ueda F, Kyoi T, Mimura K, Kimura K, Yamamoto M. Intercellular communication in cultured rabbit gastric epithelial cells. *Jpn J Pharmacol* 1991;**57:**321–328.
15. Uchida Y, Shiba H, Komatsuzawa H *et al.* Irsogladine maleate influences the response of gap junctional intercellular communication and IL-8 of human gingival epithelial cells following periodontopathogenic bacterial challenge. *Biochem Biophys Res Commun* 2005;**333:**502–507.
16. Fujita T, Ashikaga A, Shiba H *et al.* Regulation of IL-8 by Irsogladine maleate is involved in abolishment of *Actinobacillus actinomycetemcomitans*-induced reduction of gap-junctional intercellular communication. *Cytokine* 2006;**34:**271–277.
17. Ten Cate AR. The role of epithelium in the development, structure and function of the tissues of tooth support. *Oral Dis* 1996;**2:**55–62.
18. Listgarten MA. Electron microscopic features of the newly formed epithelial attachment after gingival surgery. A preliminary report. *J Periodontal Res* 1967; **2:**46–52.
19. Listgarten MA, Ellegaard B. Electron microscopic evidence of a cellular attachment between junctional epithelium and dental calculus. *J Periodontal Res* 1973;**8:** 143–150.
20. Innes PB. An electron microscopic study of the regeneration of gingival epithelium following gingivectomy in the dog. *J Periodontal Res* 1970;**5:**196–204.
21. Braga AM, Squier CA. Ultrastructure of regenerating junctional epithelium in the monkey. *J Periodontol* 1980;**51:**386–392.
22. Frank R, Fiore-Donno G, Cimasoni G, Ogilvie A. Gingival reattachment after surgery in man: an electron microscopic study. *J Periodontol* 1972;**43:**597–605.
23. Kesavalu L, Chandrasekar B, Ebersole JL. *In vivo* induction of proinflammatory cytokines in mouse tissue by *Porphyromonas gingivalis* and *Actinobacillus actinomycetemcomitans*. *Oral Microbiol Immunol* 2002;**17:**177–180.
24. Kusumoto Y, Hirano H, Saitoh K *et al.* Human gingival epithelial cells produce chemotactic factors interleukin-8 and monocyte chemoattractant protein-1 after stimulation with *Porphyromonas gingivalis* via toll-like receptor 2. *J Periodontol* 2004;**75:**370–379.
25. Coyne CB, Vanhook MK, Gambling TM, Carson JL, Boucher RC, Johnson LG. Regulation of airway tight junctions by proinflammatory cytokines. *Mol Biol Cell* 2002;**13:**3218–3234.
26. Ma TY, Boivin MA, Ye D, Pedram A, Said HM. Mechanism of TNF-{alpha} modulation of Caco-2 intestinal epithelial tight junction barrier: role of myosin light-chain kinase protein expression. *Am J Physiol Gastrointest Liver Physiol* 2005; **288:**G422–430.
27. Kimura K, Teranishi S, Fukuda K, Kawamoto K, Nishida T. Delayed disruption of barrier function in cultured human corneal epithelial cells induced by tumor necrosis factor-alpha in a manner dependent on NF-kappaB. *Invest Ophthalmol Vis Sci* 2008;**49:**565–571.
28. Shivanna M, Srinivas SP. Microtubule stabilization opposes the (TNF-alpha)-induced loss in the barrier integrity of corneal endothelium. *Exp Eye Res* 2009;**89:** 950–959.
29. Petrache I, Birukova A, Ramirez SI, Garcia JG, Verin AD. The role of the

microtubules in tumor necrosis factor-alpha-induced endothelial cell permeability. *Am J Respir Cell Mol Biol* 2003;**28:** 574–581.

30. Ma TY, Iwamoto GK, Hoa NT *et al.* TNF-alpha-induced increase in intestinal epithelial tight junction permeability requires NF-kappa B activation. *Am J Physiol Gastrointest Liver Physiol* 2004; **286:**G367–376.
31. Amasheh M, Fromm A, Krug SM *et al.* TNF{alpha}-induced and berberine-antagonized tight junction barrier impairment via tyrosine kinase, Akt and NF{kappa}B signaling. *J Cell Sci* 2010; **123:**4145–4155.
32. Baker OJ, Camden JM, Redman RS *et al.* Proinflammatory cytokines tumor necrosis factor-alpha and interferon-gamma alter tight junction structure and function in the rat parotid gland Par-C10 cell line. *Am J Physiol Cell Physiol* 2008;**295:** C1191–1201.
33. Chen C, Jamaluddin MS, Yan S, Sheikh-Hamad D, Yao Q. Human stanniocalcin-1 blocks TNF-alpha-induced monolayer permeability in human coronary artery endothelial cells. *Arterioscler Thromb Vasc Biol* 2008;**28:**906–912.
34. Fujita T, Ashikaga A, Shiba H *et al.* Irsogladine maleate counters the interleukin-1 beta-induced suppression in gap-junctional intercellular communication but does not affect the interleukin-1 beta-induced zonula occludens protein-1 levels in human gingival epithelial cells. *J Periodontal Res* 2008;**43:**96–102.
35. Carayol N, Vachier I, Campbell A *et al.* Regulation of E-cadherin expression by dexamethasone and tumour necrosis factor-alpha in nasal epithelium. *Eur Respir J* 2002;**20:**1430–1436.
36. Carayol N, Campbell A, Vachier I *et al.* Modulation of cadherin and catenins expression by tumor necrosis factor-alpha and dexamethasone in human bronchial epithelial cells. *Am J Respir Cell Mol Biol* 2002;**26:**341–347.

原　著

歯周炎罹患歯に対するFGF-2投与の長期的効果および安全性の検討

北村正博[*1]，古市保志[*2]，藤井健男[*3]，川浪雅光[*4]，國松和司[*5]，
島内英俊[*6]，山田　了[*7]，小方頼昌[*8]，和泉雄一[*9]，伊藤公一[*10]，
中川種昭[*11]，新井　高[*12]，山崎和久[*13]，吉江弘正[*14]，野口俊英[*15]，
渋谷俊昭[*16]，高柴正悟[*17]，栗原英見[*18]，永田俊彦[*19]，横田　誠[*20]，
前田勝正[*21]，廣藤卓雄[*22]，坂上竜資[*23]，原　宜興[*24]，野口和行[*25]，
小笠原健文[*26]，村上伸也[*1]

[*1]大阪大学大学院歯学研究科口腔分子免疫制御学講座歯周病分子病態学
[*2]北海道医療大学歯学部口腔機能修復・再建学系 歯周歯内治療学分野
[*3]北海道医療大学歯学部口腔機能修復・再建学系高度先進保存学分野
[*4]北海道大学大学院歯学研究科口腔健康科学講座歯周・歯内療法学教室
[*5]医療法人社団 顕正会歯科臨床研修センター
[*6]東北大学大学院歯学研究科口腔生物学講座歯内歯周治療学分野
[*7]東京歯科大学
[*8]日本大学松戸歯学部歯周治療学講座
[*9]東京医科歯科大学大学院医歯学総合研究科歯周病学分野
[*10]日本大学歯学部保存学教室歯周病学講座
[*11]慶應義塾大学病院歯科・口腔外科教室
[*12]鶴見大学歯学部第二歯科保存学教室
[*13]新潟大学大学院医歯学総合研究科口腔生命福祉学専攻口腔生命福祉学科口腔保健学講座
[*14]新潟大学大学院医歯学総合研究科摂食環境制御学講座歯周診断・再建学分野
[*15]愛知学院大学歯学部歯周病学講座
[*16]朝日大学歯学部口腔感染医療学講座歯周病学分野
[*17]岡山大学大学院医歯薬学総合研究科病態制御科学専攻病態機構学講座歯周病態学分野
[*18]広島大学大学院医歯薬学総合研究科先進医療開発科学講座歯周病態学分野
[*19]徳島大学大学院ヘルスバイオサイエンス研究部歯周歯内治療学分野
[*20]九州歯科大学
[*21]九州大学大学院歯学研究院口腔機能修復学講座歯周病学分野
[*22]福岡歯科大学総合歯科学講座総合歯科学分野
[*23]福岡歯科大学口腔治療学講座歯周病学分野
[*24]長崎大学大学院医歯薬学総合研究科医療科学専攻展開医療科学講座歯周病学分野
[*25]鹿児島大学大学院医歯学総合研究科先進治療科学専攻顎顔面機能再建学講座歯周病学分野
[*26]町田市民病院　歯科・歯科口腔外科

（受付日：2011年11月14日　受理日：2012年1月28日）

連絡先：村上伸也
〒565-0871 大阪府吹田市山田丘1-8
大阪大学大学院歯学研究科口腔分子免疫制御学講座歯周病分子病態学
Shinya Murakami
Department of Periodontology, Division of Oral Biology and Disease Control, Osaka University Graduate School of Dentistry
1-8, Yamadaoka, Suita, Osaka 565-0871, Japan
E-mail：ipshinya @dent.osaka-u.ac.jp